

**COMPUTER VISION AND MACHINE LEARNING BASED
ADAPTABLE CONVERSION METHOD
FOR ANY LIGHT MICROSCOPE TO AUTOMATED CELL COUNTER
BY TRYPAN BLUE DYE-EXCLUSION**

A DOCTOR OF PHILOSOPHY THESIS

in

Software Engineering

Atılım University

by

AKIN ÖZKAN

JULY 2017

**COMPUTER VISION AND MACHINE LEARNING BASED
ADAPTABLE CONVERSION METHOD
FOR ANY LIGHT MICROSCOPE TO AUTOMATED CELL COUNTER
BY TRYPAN BLUE DYE-EXCLUSION**

**A THESIS SUBMITTED TO
THE GRADUATE SCHOOL OF NATURAL AND APPLIED SCIENCES
OF
ATILIM UNIVERSITY
BY
AKIN ÖZKAN**

**IN PARTIAL FULFILLMENT OF THE REQUIREMENTS FOR THE
DEGREE OF**

DOCTOR OF PHILOSOPHY

IN

THE DEPARTMENT OF SOFTWARE ENGINEERING

JULY 2017

Approval of the Graduate School of Natural and Applied Sciences, Atılım University.

Prof. Dr. Ali Kara
Director

I certify that this thesis satisfies all the requirements as a thesis for the degree of Doctor of Philosophy.

Prof. Dr. Ali Yazıcı
Head of Department

This is to certify that we have read the thesis “**Computer Vision And Machine Learning Based Adaptable Conversion Method For Any Manual Light Microscope To Automated Cell Counter By Trypan Blue Dye-Exclusion**” submitted by “**Akın Özkan**” and that in our opinion it is fully adequate, in scope and quality, as a thesis for the degree of Doctor of Philosophy.

Asst. Prof. Dr. Gökhan Şengül
Co-Supervisor

Assoc. Prof. Dr. S. Belgin İşgör
Supervisor

Examining Committee Members

Assoc. Prof. Dr. Sedat Nazlıbilek

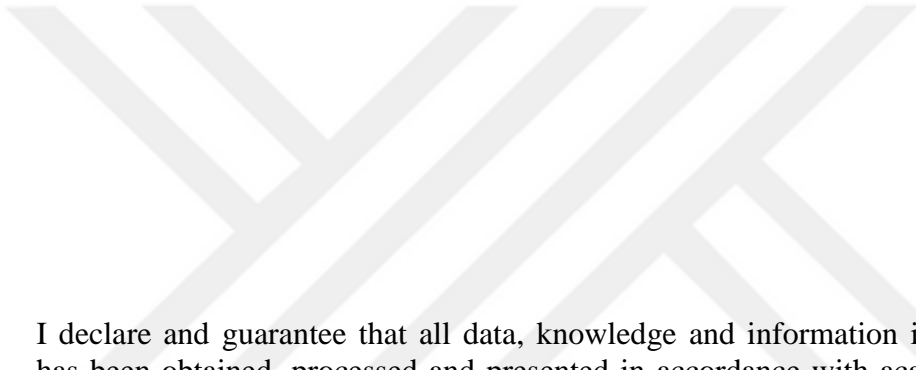
Assoc. Prof. Dr. S. Belgin İşgör

Assoc. Prof. Dr. Yasemin G. İşgör

Assoc. Prof. Dr. Nergiz E. Çağiltay

Prof. Dr. Serpil Oğuztüzün

Date: July 10, 2017



I declare and guarantee that all data, knowledge and information in this document has been obtained, processed and presented in accordance with academic rules and ethical conduct. Based on these rules and conduct, I have fully cited and referenced all material and results that are not original to this work.

Name, Last name: Akın Özkan

Signature:

ABSTRACT

COMPUTER VISION AND MACHINE LEARNING BASED ADAPTABLE CONVERSION METHOD FOR ANY LIGHT MICROSCOPE TO AUTOMATED CELL COUNTER BY TRYPAN BLUE DYE-EXCLUSION

Özkan, Akın

Ph.D., Software Engineering Department

Supervisor: Assoc. Prof. Dr. S. Belgin İşgör
Co-Supervisor: Asst. Prof. Dr. Gökhan Şengül

July 2017, 80 pages

Almost all of the cell biology experiments involve counting of cells regularly to monitor cell proliferation and viability. Knowledge of the cell quantity and quality are important parameters for the experimental standardization and toxicity impact estimation. There are two different approaches to count the cells, such as, hemocytometer-based manual counting, and usage of an automated cell counter. Either of the methods have their advantages and disadvantages. High investment and operational cost limit the wide range usage of automated cell counters. On the other hand, manual cell counting based on hemocytometer has various limitations by the fact that reliability of cell counting highly depends on operator's experience. Moreover, high estimation time requirement and human labor are two more drawbacks of the manual process. This thesis proposes state-of-the-art alternative method (i.e. framework) for the cell counting by defining computer vision and machine learning based conversion methodology. The basis of the proposed method is the adaptation of hemocytometer-based manual counting to automated procedure by adding middleware decision software to reduce its shortcomings. In addition, two novel data sets are collected to test our proposed method in terms of cell counting (i.e. non-stained) and cell viability analysis (i.e. stained). The datasets are available for non-profit public usage from "biochem.atilim.edu.tr/datasets/" which will be baseline to future studies on this research domain. Both datasets contain two different types of

cancer cell images, namely, *caucasian promyelocytic leukemia* (HL60), and *chronic myelogenous leukemia* (K562). From our experimental results, our method reaches up to 92% and 74% in terms of recall scores for HL60 and K562 cancer cells, respectively, with the high precision. The experimental results also validate that the proposed method can be a powerful alternative to the current cell counting approaches.

Keywords: Cell counting, cell viability, light microscope, hemocytometer, HL60, K562



ÖZ

BİLGİSAYARLI GÖRME VE MAKİNE ÖĞRENME'YE DAYALI OLARAK TRAPAN MAVİSİ BOYA DIŞLAMA TABANLI IŞIK MİKROSKOPLARININ OTOMATİZE HÜCRE SAYARINA UYARLANABİLİR DÖNÜŞÜM YÖNTEMİ

Özkan, Akın

Doktora, Yazılım Mühendisliği Bölümü

Tez Yöneticisi: Doç. Dr. S. Belgin İşgör
Ortak Tez Yöneticisi: Yrd. Doç. Dr. Gökhan Şengül

Temmuz 2017, 80 sayfa

Hücre biyolojisi deneylerinin hemen hemen hepsi, hücre çoğalmasını ve yaşayabilirliğini izlemek için düzenli olarak hücrelerin sayımını içerir. Hücrenin miktarı ve kalitesinin bilgisi, deneysel standardizasyon ve toksisite etkisi tahmini için önemli parametrelerdir. Hücreleri saymak için hemositometre tabanlı elle sayma ve otomatik hücre sayacının kullanımı gibi iki farklı yaklaşım vardır. Yöntemlerden her ikisinin de avantajları ve dezavantajları vardır. Yüksek yatırım ve operasyonel maliyet otomatik hücre sayaçlarının geniş kullanımını sınırlar. Öte yandan, hemositometreye dayalı manuel hücre sayımı, hücre sayımının güvenilirliğinin, operatörün deneyimine ve yorgunluğuna büyük ölçüde bağlı olduğu gerçeği ile çeşitli sınırlamaları vardır. . Uzun zaman gereksinimi ve insan işgücü elle işleme sürecinin iki dezavantajı olarak sayılabilir. Bu tez, görüntü işleme ve makine öğrenmeyi esas alan dönüştürme metodolojisini tanımlayarak hücre sayımı için en gelişmiş alternatif metodu (çerçeve iskeleti) önermektedir. Önerilen yöntemin temelini, eksikliklerini azaltmak için ara katman karar yazılımı ekleyerek elle sayım yöntemine hemocytomer tabanlı otomatik saymanın uyarlanmasıdır. Buna ek olarak, önerilen yöntemimizi hücre sayımı (boyasız) ve hücre yaşayabilirliği analizi (boyalı) açısından test etmek için iki yeni veri seti toplanmıştır. Bu veri kümeleri, "biyokimyasal.atilim.edu.tr/datasets/" adresinden kâr amacı gütmeyen herkesin kullanımına sunulmaktadır ve bu da bu araştırma alanındaki gelecek çalışmalara

temel teşkil edecektir. Her iki veri kümesi, iki farklı türde kanser hücresi görüntüsü, yani, beyaz renkli promiyelositik lösemi (HL60) ve kronik miyelojenik lösemi (K562) içerir. Deneysel sonuçlarımızdan yola çıkarak, yöntemimiz HL60 ve K562 kanser hücreleri için sırasıyla geri çağırma skorları açısından % 92 ve % 74'e kadar ulaşmaktadır. Deney sonuçları, önerilen yöntemin mevcut hücre sayımı yaklaşımlarına güçlü bir alternatif olabileceğini de doğrular.

Anahtar Kelimeler: Hücre sayımı, hücre canlılık analizi, ışık mikroskopisi, hemositometre, HL60, K562





To My Parents

ACKNOWLEDGMENTS

First and foremost I would like to express my sincere gratitude to my supervisors Assoc. Prof. Dr. S. Belgin İşgör and Asst. Prof. Dr. Gökhan Şengül for their valuable advises, support, guidance, insight, patience, and encouragement throughout the study.

I express sincere appreciation to my thesis progress jury members, Assoc. Prof. Dr. Yasemin G. İşgör and Assoc. Prof. Dr. Sedat Nazlıbilek for their criticism, guidance, and suggestions.

I am thankful to my thesis jury members, Doç. Dr. Nergiz E. Çağıltay and Prof. Dr. Serpil Oğuztüzün for their evaluations and future instructions.

A part of this study was accomplished using Atılım University Cell Biology laboratory. I would like to additionally thank Assoc. Prof. Dr. S. Belgin İşgör and Assoc. Prof. Dr. Yasemin G. İşgör for providing the cells and also for their hands-on laboratory guidance.

I am also grateful to Atılım University, the head of Software Engineering Department, Prof. Dr. Ali Yazıcı for his support.

I would like to thank TÜBİTAK (The Scientific and Technological Research Council of Turkey) for supporting my thesis via 2211-C Domestic Doctorate Scholarship Program Intended for Priority Areas (No. 1649B031500060).

Finally, I owe special thanks to my family, my mother Serap Özkan, my father Arif Özkan and my brother Savaş Özkan for their unconditioned support and endless patience. It is great to know that they will be always with me whenever I need a help.

TABLE OF CONTENTS

| | |
|---|-----|
| ABSTRACT | iv |
| ÖZ | vi |
| ACKNOWLEDGMENTS | ix |
| LIST OF FIGURES | xiv |
| LIST OF ABBREVIATIONS | xvi |
| CHAPTER | |
| 1. INTRODUCTION | 1 |
| 1.1. Materials in Cell Biology | 2 |
| 1.1.1. Cell Culture Incubator | 2 |
| 1.1.2. Biological Safety Cabinet | 3 |
| 1.1.3. Hemocytometer | 4 |
| 1.1.4. Light Microscope | 6 |
| 1.2. Methods in Cell Biology | 7 |
| 1.2.1. Cell Passaging | 8 |
| 1.2.2. Manual Cell Counting by Hemocytometer | 9 |
| 1.2.3. Manual Cell Viability (Dye-exclusion)..... | 10 |
| 1.3. Toxicology and Anticancer Drug Discovery Studies | 12 |
| 1.4. Problem Definition | 13 |
| 1.5. Contributions | 15 |
| 1.6. Organization | 16 |
| 2. RELATED WORKS | 17 |
| 2.1. Automated Cell Counting..... | 19 |

| | |
|---|----|
| 2.2. Automated Cell Viability Analysis | 22 |
| 3. SOFTWARE ENGINEERING | 25 |
| 3.1. Requirement Analysis | 25 |
| 3.2. Quality Checking..... | 26 |
| 3.3. Software Process Model..... | 27 |
| 3.4. Algorithmic Complexity..... | 28 |
| 4. TECHNICAL METHODOLOGIES | 31 |
| 4.1. Feature Extractors..... | 31 |
| 4.1.1. Local Binary Patterns (LBP)..... | 32 |
| 4.1.2. Local Phase Quantization (LPQ) | 33 |
| 4.1.3. Histogram Oriented Gradients | 33 |
| 4.2. Classifiers | 34 |
| 4.2.1. K-Nearest Neighbor (KNN)..... | 35 |
| 4.2.2. Support Vector Machines (SVM) | 36 |
| 4.2.2.1. Data Separability..... | 37 |
| 4.2.2.2. Kernel trick..... | 38 |
| 4.2.3. Random Forests (RF) | 38 |
| 4.3. Cross Validation | 40 |
| 4.4. Sliding Window..... | 41 |
| 4.5. Bounding Box Collision..... | 42 |
| 5. PROPOSED METHOD | 43 |
| 5.1. Acquired Image Datasets..... | 43 |
| 5.1.1. HL60_HEM40x_CC | 44 |
| 5.1.1.1. Image Datasets | 44 |
| 5.1.1.2. Ground Truth Locations Data | 45 |
| 5.1.1.3. Region of Interest (ROI) Boundary Location Data..... | 46 |
| 5.1.2. HL60_K512_HEM40X_CV | 46 |

| | |
|---|----|
| 5.1.2.1. Annotation Strategy | 47 |
| 5.2. STAGE 1: Cell Location Finding Pipeline..... | 48 |
| 5.2.1. Improve Image Quality | 49 |
| 5.2.2. Defining the ROI..... | 50 |
| 5.2.3. Reducing Search Space | 50 |
| 5.2.4. Finding Cell Locations | 51 |
| 5.2.5. Elimination of the Nested Cell Locations | 52 |
| 5.3. STAGE 2: Automated Cell Viability Analysis | 54 |
| 5.4. STAGE 3: Overall Proposed Method..... | 54 |
| 6. EXPERIMENTAL RESULTS AND DISCUSSION..... | 56 |
| 6.1. Performance Metrics | 56 |
| 6.2. Method Performance Evaluation Routine | 57 |
| 6.3. Proposed Cell Counting Pipeline Performance | 58 |
| 6.4. Proposed Automated Cell Viability Analysis Performance | 61 |
| 6.5. Overall Method Results | 67 |
| 7. CONCLUSIONS | 69 |
| REFERENCES..... | 71 |

LIST OF TABLES

TABLE

| | |
|--|----|
| 1. Obtained data for each publication | 17 |
| 2. Number of annotated HL60 cells for cell location finding (stage 1) | 45 |
| 3. Number of annotated HL60 and K562 cell images..... | 47 |
| 4. Sample confusion matrix | 56 |
| 5. The best parameters for cell location finding..... | 59 |
| 6. Cell location finding results by Min Type bounding box with threshold 0.8 | 60 |
| 7. Cell location finding results by Min Type bounding box with threshold 0.9 | 60 |
| 8. Considered classifier parameters and intervals | 61 |
| 9. Considered feature extractor parameters and intervals | 62 |
| 10. Obtained the lowest misclassification rates for HL60 | 66 |
| 11. Obtained the lowest misclassification rates for K562..... | 66 |
| 12. Automated cell viability results for HL60 by Min Type bounding box with threshold 0.8..... | 67 |
| 13. Automated cell viability results for K562 by Min Type bounding box with threshold 0.8..... | 67 |
| 14. Automated cell viability results for HL60 by Min Type bounding box with threshold 0.9..... | 68 |
| 15. Automated cell viability results for K562 by Min Type bounding box..... | 68 |

LIST OF FIGURES

FIGURE

| | |
|---|----|
| 1. Cell culture incubator | 3 |
| 2. Biological safety cabinet | 4 |
| 3. Hemocytometer and counting chambers | 5 |
| 4. Hemocytometer side view | 5 |
| 5. Sample images using different microscope magnification values. From left to right, top to bottom: empty 4x, 10x, 40x magnifications, non-empty 40x | 7 |
| 6. Typical cell growth curve | 8 |
| 7. Cell passaging | 8 |
| 8. Conventional rule to avoid double-counting using hemocytometer. | 9 |
| 9. Dye-exclusion principle by trypan blue. (Left) alive cell, (Right) dead cell | 10 |
| 10. Randomly selected viable and non-viable cell samples from our image datasets. a) H160 alive cells b) H160 dead cells c) K562 alive cells d) K562 dead cells | 11 |
| 11. Typical anticancer drug discovery experiment flow | 14 |
| 12. Our preliminary iterative research strategy | 18 |
| 13. Automated cell counting literature | 19 |
| 14. Automated cell viability literature | 22 |
| 15. Spiral software process model | 27 |
| 16. Time complexity analysis (number of windows versus required time) | 30 |
| 17. Example of LBP using 3x3 window | 32 |
| 18. LBP circular neighborhood | 32 |
| 19. The flow of HOG | 34 |
| 20. Example of KNN in two dimensional (2D) space | 36 |
| 21. a) Possible solutions for SVM b) the best possible strength line | 36 |
| 22. a) linearly seperable data b) non-linearly separable data | 37 |
| 23. SVM kernel trick | 38 |

| | |
|---|----|
| 24. The tree has three types of node; root node (red), internal node (blue), leaf or terminal node (green) | 39 |
| 25. Random forest | 40 |
| 26. Sliding window | 42 |
| 27. Randomly chosen sample images from our novel dataset those have possible adverse conditions | 45 |
| 28. A sample image from the dataset with corresponding ground truth annotations by experts. Cell locations (green), ROI boundary location data (blue). | 46 |
| 29. Image annotation strategy | 48 |
| 30. Cell counting pipeline | 49 |
| 31. The flow chart for cell location finding | 51 |
| 32. Example of cell location finding pipeline a) Input image b) defining the considered area (green square) c) contrast enhancement d) decide the possible cell locations using edginess e) shrinking the cell search space f) find cell locations g) Elimination of the nested cell locations e) cell locations output list..... | 53 |
| 33. Proposed light microscope to vision based cell analyzer (Stage3) | 55 |
| 34. Method performance evaluation flow chart | 58 |
| 35. Misclassification rates for HL60 using various parameters of LBP | 63 |
| 36. Misclassification rates for HL60 using various parameters of LPQ | 64 |
| 37. Misclassification rates for HL60 using various parameters of LBP | 64 |
| 38. Misclassification rates for K562 using various parameters of LBP..... | 65 |
| 39. Misclassification rates for K562 using various parameters of LPQ | 65 |
| 40. Misclassification rates for K562 using various parameters of HOG | 65 |

LIST OF ABBREVIATIONS

| | | |
|-----------------|---|----------------------------------|
| HL60 | - | Caucasian promyelocytic leukemia |
| K562 | - | Chronic myelogenous leukemia |
| TB | - | Trypan blue |
| LBP | - | Local binary pattern |
| LPQ | - | Local phase quantization |
| HOG | - | Histogram oriented gradients |
| mL | - | Milliliter |
| CO ₂ | - | Carbon dioxide |

CHAPTER 1

INTRODUCTION

Light microscope and hemocytometer based manual cell counting and cell viability analysis has been broadly used in cell biology [1] including, toxicology and drug discovery studies. Moreover, this process may unveil information about the condition of cell population and cell density to understand concerning cell culture's condition to examiner. Cells are mostly counted manually by experts using light microscopy [2]. During the manual counting process, there are two main problems including its time consuming task and also its accuracy changing with experience of the examiners including with the tiredness of examiner [3]. As a result of these, automated cell counting and viability analysis will be very useful tool to improve accuracy and decrease timing of counting procedure. There are various commercial automated cell counting products yet their high cost limits the wide usage. This study presents overall methodology for automated cell location finding (i.e. counting) pipeline and automated cell viability analysis using light microscope images based on hemocytometer.

Proposed method includes three complementary research stages: cell counting (stage1), viability analysis (stage2), and overall system definition (stage3). In the first stage, automated cell location finding (i.e. cell counting) pipeline is addressed. After the satisfactory performance is reached for the first stage, automated cell viability analysis research is initiated as a second research stage. In the last stage, a resulted method has been introduced by combining the previous two stages.

The rest of the introduction chapter is organized as follows. Section 1.1 and Section 1.2 introduces materials and methods, respectively that are used in cell biology

including cancer drug discovery. Section 1.3 describes cancer drug discovery studies to define scope of the thesis. Section 1.4 reveals the main problems and the aim of the thesis. Section 1.5 outlines the contributions of the thesis. Section 1.6 explains organization of the thesis.

1.1. Materials in Cell Biology

There are several common equipment in cell biology laboratories [4]. This section lists the equipment only directly related to the thesis. Particularly, certain type of tools using throughout the cell experiments to avoid any bacterial contamination and to ensure the suitable environmental conditions. Additionally, manual cell counting and viability analysis requires three essential equipments, such as, microscope, hemocytometer, and the trypan blue dye.

1.1.1. Cell Culture Incubator

Cell cultures are grown using medium in flasks with the help of the incubator [5]. Flasks can be defined as a plastic plate to cover cells and needed material (i.e. medium). Medium is the liquid that contain all required nutrients used to grow cells outside of their natural environment. They are stored in the incubator to control the essential environmental conditions, such as, temperature level, moisture range, and carbon dioxide (CO₂) percentage etc.

Temperature in an incubator is usually controlled by electric coils that produce heat. Humidity is maintained by a water reservoir placed at the bottom of the incubator. Since CO₂ level is vital to maintain optimum pH in medium, it should be supplied from external source in control. A cell culture incubator is designed to maintain a constant temperature and high humidity for the growth of tissue culture cells under a CO₂ atmosphere. Generally, cells achieve optimal growth tendency in an incubator at a temperature of 37°C and under 95-98% humidity with 5% CO₂.

The incubator have been used in our laboratory is shown in Figure 1. Normally the door of the incubator is always closed and it opens only the required cases under rigorous protocols to preserve cell cultures from any bacterial contamination. It

shelters several flasks during the cell experiments and they contain cells in medium which the color seems pinky.



Figure 1. Cell culture incubator

1.1.2. Biological Safety Cabinet

Biological safety cabinets or cell culture hoods are preliminary designed to ensure two groups of protection [6] as follows:

- Operator (i.e. researcher) protection from dangerous contagious materials inside the cabinet.
- Cell culture protection to prevent any bacterial contamination causing by partials that flows in the air.

Inside of the hood should constantly be cleared by the operator with the 70% ethanol before usage to ensure aseptic work area. Additionally, each and every required item is sterilized by 70% ethanol before placed in the cell culture hood. There are different classes and types of them which produce various degrees of protection from 1 to 4 based on hazard level of the used cell culture and the experimental essence.

Biological safety cabinet (Figure 2) maintains a constant, unidirectional flow of filtered air over the work area in the interior. Since the interior space of cabinet are limited, working area layout is important. Conventionally, needed gadgets that are inside of the hood are organized from clean (i.e. Less contaminated) to dirty (higher contaminated). By doing this alignment, it guaranties that the direction of workflow goes from the clean side to the dirty side.



Figure 2. Biological safety cabinet

1.1.3. Hemocytometer

Despite the current technological development of cell biology researches, hemocytometer [7] based cell counting and viability analysis are still the most widespread method in the world. It was first developed to estimate the number of blood cells in unit volume but became an indispensable tool for cell biology

laboratories to count a variety of other cell types, including, cancer cells. There are few different counting chambers on market. Main differences are their size of counting area, their location of the lines with respect to each other and thickness of lines.

Hemocytometer (i.e. improved hemocytometer) is square-shaped glass equipment which includes two counting chambers on it as shown in the Figure 3. Each chamber has 1x1mm counting area marked by repetitive uniform bold white lines [8]. With the help of these lines, examiner prevent the consideration of same cells again and again while investigation.

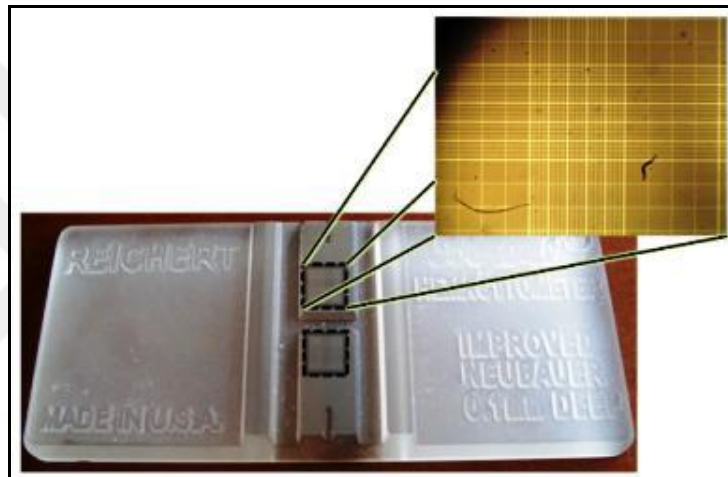


Figure 3. Hemocytometer and counting chambers

Additionally, each chamber of the hemocytometer contains particular volume of solution with cover slip in place that is volume of 0.1mm^3 or 10^{-4}cm^3 (Figure 4). Using count of cell sample, cells/ml can be calculated for getting information about over all cell suspension. Since, each chamber is quantitatively identical and represents an exact volume of sample with cover slip (1 mL), the total number of cells can be estimated for cell culture which cell sample was taken.

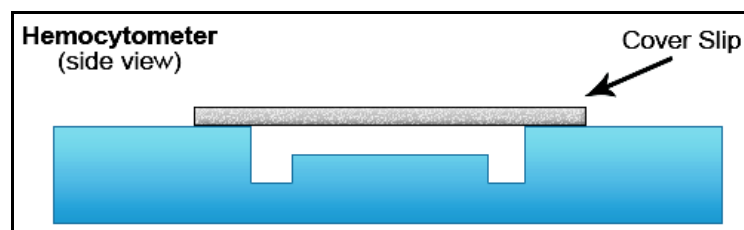


Figure 4. Hemocytometer side view

Before the manual counting process, cell suspension sample has to be diluted to get the cell density low enough for the reliable counting. When this happens final counting result has to be multiplied by the dilution factor (1). Depending on cell culture type, dilution level can be adjusted to obtain suitable concentration. Typically, cell suspension sample should be diluted that each square does not have more than 10 cells to make counting process more easy and consistent.

Cell concentration will be determined using the following equation:

$$\text{Total cell number} = A \times D \times 10^4 \times O \quad (1)$$

where;

- A is the average count per square
- D is the dilution factor
- O is the original volume of cell suspension which cell sample was taken

1.1.4. Light Microscope

Microscope [9] is a fundamental instrument for analyzing the structure and function of biological specimens. Also, images of the inspected specimen can be acquired with the help of a camera that is attached to the microscope and can be transferred to the computer for further processing. According to their basic operating fundamentals, there are various kinds of microscopes available, such as, bright-field, dark-field, fluorescence and, phase contrast. Our proposed solution mainly targets light microscope. Even if light microscopes are not adequately powerful to show cell organization with all the details, they are mostly used microscope type due to their low price.

Light microscopes are basically the type of microscope in which the light source is at the bottom and the objective is at the top and the sample that will be examined is placed between these two [10]. The light beam passes through the sample and reaches the objective. There are several different magnification values using objective in microscopes, and the researcher can instantly change this value according to his needs. The cell sample can be examined by the investigator for

different magnifications (4x, 10x, 40x, 100x and so). Depending on the increase of the magnification value, the detail of the view increases but the visible area decreases as shown in Figure 5. For this reason, the magnification value to be used can be different according to the cell samples. In some cases, it may be necessary to examine the same cell sample with a different magnification values. The 40x lens setting is often used during cell counting [11]. For this reason, images taken using the 40x magnification value are considered in this study.

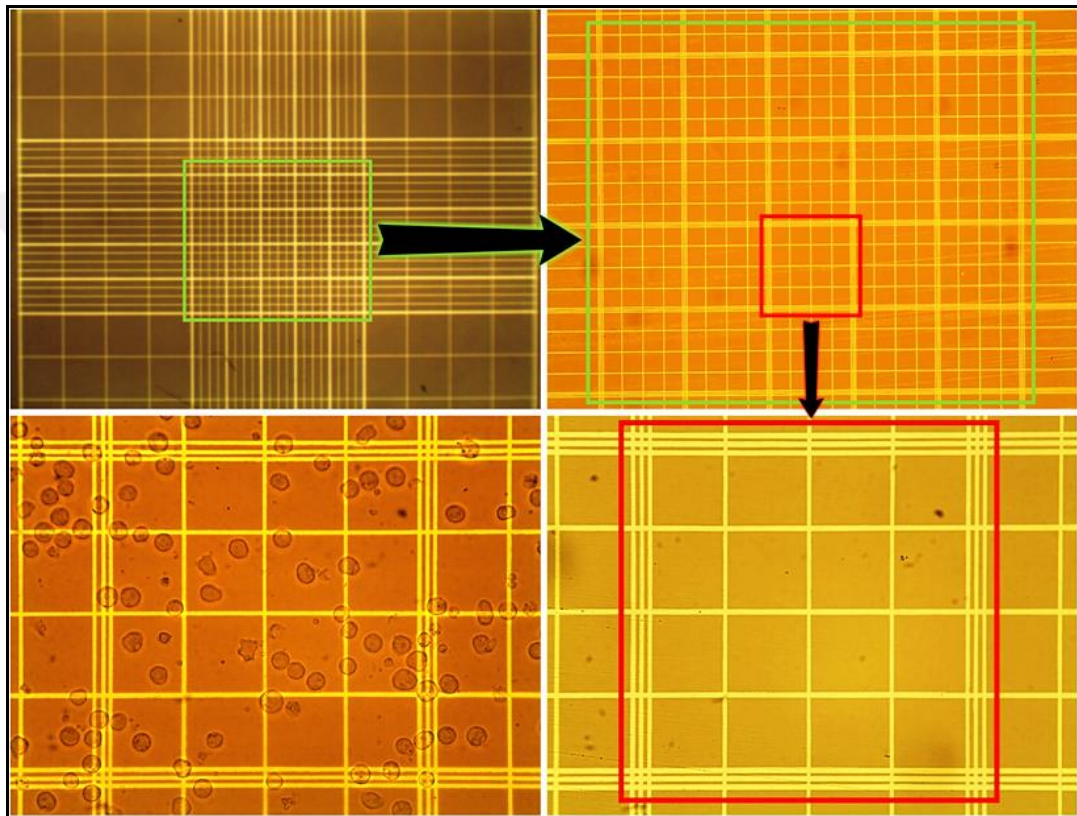


Figure 5. Sample images using different microscope magnification values. From left to right, top to bottom: empty 4x, 10x, 40x magnifications, non-empty 40x

1.2. Methods in Cell Biology

There are different set of protocols. This chapter provides basic knowledge of cell biology methods as a guidance of cell laboratory protocols. The following methods highlight the most common techniques used in cell biology. This section describes how to perform a manual cell counting, in order to achieve consistent results.

1.2.1. Cell Passaging

Growth of cells in culture follows a standard pattern called the growth curve [12]. Maintaining growth curve will maximize the number of healthy cells for your experiment and it will directly affect the quality of experimental work. The typical growth curve of cells in a culture is illustrated in Figure 6. The initial lag phase is followed by log phase and a plateau phase. During the growth period in the log phase, the medium must be renewed regularly. Constantly, the number of cells in a medium should be transferred into new and fresh plates (i.e. flask) when the cell density exceeds the capacity of the medium.

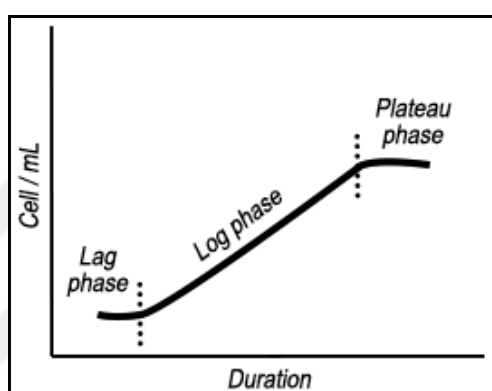


Figure 6. Typical cell growth curve

The division of cell culture into fresh medium (Figure 7) called sub-culturing is also referred to as cell passaging [13] which enables the further propagation of the cell culture based on log phase principle. The cell passaging procedure takes place inside the biological safety cabinet. Also, passage number is marked on a flask to indicate the number of times a cell culture has been sub-cultured.

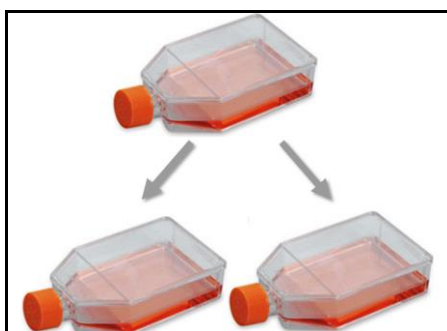


Figure 7. Cell passaging

1.2.2. Manual Cell Counting by Hemocytometer

Cell counting procedure is an indispensable part of cell culture experiments [14]. Cell counting helps to maintain density of cell culture for optimal growth. Additionally, knowledge of considered cell quantity is an important parameter for cell based experiments. Starting with an accurate cell amount supports and guarantees the correct experimental results. The cells are counted manually by the researchers using hemocytometer under microscope. The counting process is completed by scanning the area on the hemocytometer under microscope. In a usual counting procedure, the central area of hemocytometer is considered as a main zone. Furthermore, there is a conventional rule [15] that has to apply to avoid double-counting. That is illustrated in Figure 8.

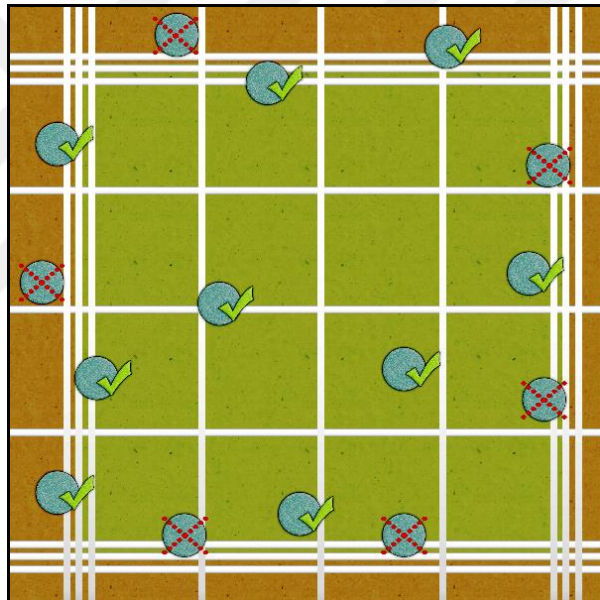


Figure 8. Conventional rule to avoid double-counting using hemocytometer.

Cells intersecting left and top sides of the middle of the triple lines are counted, however cells on the right and bottom ones are not counted. While manual counting, indirectly, region of interest (ROI) defines using this rule. Generally, different laboratories have diverse number of counting protocols, but the similar types of routines are preserved [16].

1.2.3. Manual Cell Viability (Dye-exclusion)

Dye-exclusion based cell viability analysis [17] has been broadly used in cell biology including anticancer drug discovery studies. Viability analysis refers to whole decision making process for the distinction of dead cells from alive ones. Basically, cell culture samples are dyed with a special stain called trypan blue, so that the dead cells are selectively colored to bluish. This distinction provides critical information that may use for unveil condition of considered cell culture or expose influences of studied drug on disease cell culture including cancer. Generally, the number of dead cells gets increased when their environment is unsuitable to live.

Although there are various stain types available for cell viability analysis, trypan blue [18] is the most commonly used type of stain to distinguish live cells from the dead ones. Trypan blue stain is helpful to identify cell viability depending on dye-exclusion [19] principle.

According to the dye-exclusion principle, trypan blue stain cannot enter inside the live cells (i.e. viable cells) but dead cells (i.e. non-viable cells) let the stain go inside because of their damaged cell membrane. Therefore, trypan blue only stains the dead cells while the alive exclude the dye (Figure 9).

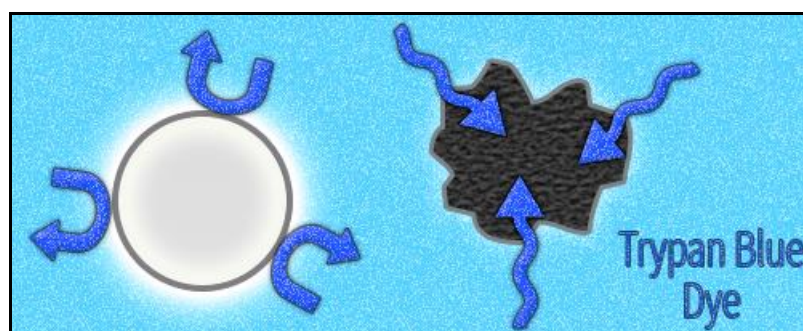


Figure 9. Dye-exclusion principle by trypan blue. (Left) alive cell, (Right) dead cell

Consequently, viable cells appear round and brighter but non-viable cells look ragged and much darker during evaluation process by expert. Sample of viable and non-viable cells encountered in this study are given in Figure 10.

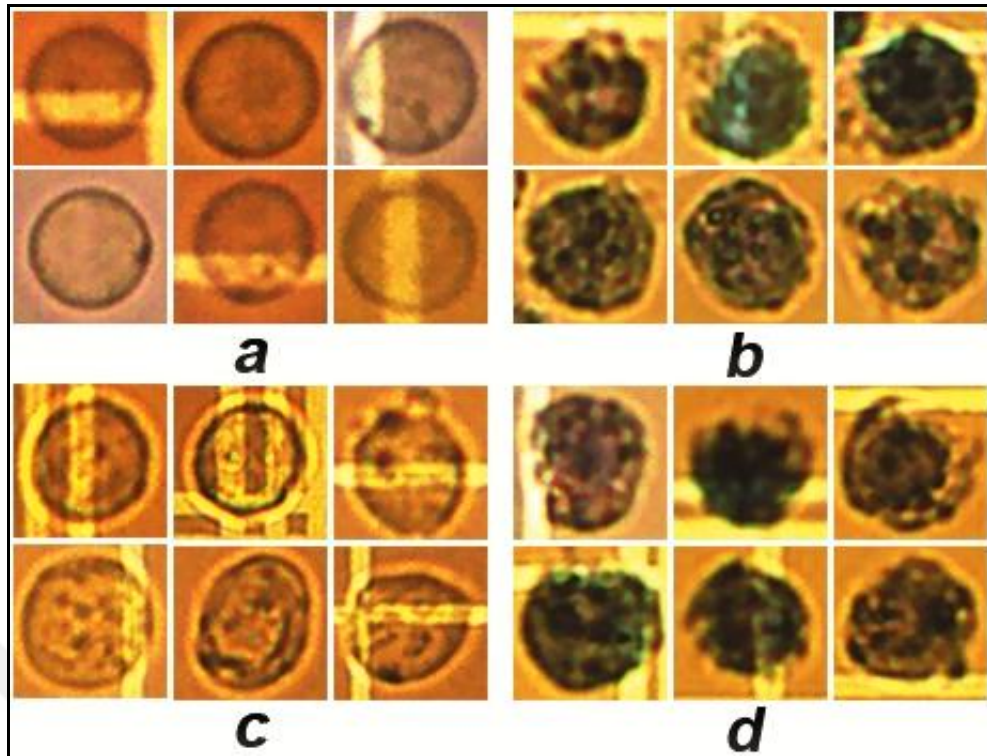


Figure 10. Randomly selected viable and non-viable cell samples from our image datasets. a) H160 alive cells b) H160 dead cells c) K562 alive cells d) K562 dead cells

In order to attain consistent and reliable accuracy from manual viability analysis, intervention should be carefully carried out by experts. Mainly, variation of the experience level and the tiredness of examiners make the process error-prone. Inevitably, this bottleneck unveils the importance of an automated solution for cell viability analysis to replace the conventional manual process.

During the decision of the cell viability, particularly, three major criteria are carefully investigated by experts. Those criteria are given as follows:

- **Condition of cell interior:** The membrane of a cell separates and protects the interior of cell from the outside surroundings by being selectively permeable. Cell death occurs when the cell membrane is damaged irreversibly. As a result of incapable cell membrane, the dead cell samples let the dye inside and its color gets noisy and darker. This interior color change yields a very important distinctive visual sign to justify the cell viability.

- **Condition of cell shape:** Even though formal deformations are observed due to their presence in the liquid medium, the two considered cancer cell types are both morphologically circular. Unusual changes in the shape of the cell and the indentation of the outer surface may also indicate cell death. This morphological change may also give information about the cell viability.
- **Condition of cell exterior:** Alive cells create a halo around their cell membrane while strives to exclude dye. Basically, halo is formed as a result of the exclusion of the stain which the flow of fluid around the cell is accelerated. On the contrary, halo could not occur around the dead cells since there is no interaction or resistance to stain.

1.3. Toxicology and Anticancer Drug Discovery Studies

Cancer can be defined as an abnormal and uncontrolled way of cell growths [20]. Mostly, it starts due to gene changes by incurring the adverse external factors or based on genetic inheritance. There are a lot of different types of cancers and they can be grouped according to the type of cell they start in, such as, leukemia. It is the name given to a group of blood cancers which is developed in the bone marrow and causes large numbers of abnormal blood cells. Leukemia is a condition in which the bone marrow makes too many white blood cells. The higher level of abnormal blood cells can make it harder for the body to get oxygen to its tissues or fight infections. Leukaemia is occupying 3 out of 100 of all cancer cases (i.e.3%) but it is the most common cancer in children [21].

Anticancer drug discovery researches span both chemical and biological experimental processes. Most of the related studies have focused on the cytotoxic agent that is driven by target-based methodologies [22]. Those studies aim to find effective extracts that have significant cytotoxic activity on cancer.

There are two accepted regulator authorities in the world for the authorization of medicinal products, namely Food and Drug Administration (FDA) and European Medicines Agency (EMA). There are similarities and differences between these two agencies in several key areas of concern for anticancer drug development. But the both agencies have the similar magnification of ensuring that safe, effective and high

quality medicines could quickly be made available. The FDA drug approval process has been taken into consideration during this study.

According to FDA, cancer drug discovery studies involve five consecutive set of research stages [23] in two periods, such as, preclinical, and clinical. It is passed to the next period when a satisfactory success is achieved. Also, the typical development duration is 10-15 years [24]. Preclinical period implies the evaluation of potential drug-extract in cells and animals respectively. Clinical period covers experiments that use human subjects to see whether a drug is effective, and what side effects it may cause.

Once a considered (i.e. lead) extract has been established, preclinical period will be started for the compound as a candidate drug. Extracts are an essence of substances as an important source of cytotoxic material. The extract can be derived from different substances, including plants, fungus, or many others. A preclinical period involves in vitro testing followed by in vivo testing to reveal safety and efficacy of extract before clinical period starts.

In vitro (Latin for “within the glass”) [25] refers to the technique of performing a given procedure in a controlled and artificial environment outside of a living organism such as petri dish, plates, or flask. In vitro conditions are usually intentionally simplified. In vivo (Latin for “within the living”), in contrast, indicates an experiment carried out using a whole, living organism such as, mice, rabbit, or apes.

1.4. Problem Definition

The complexity of interpreting huge number of image data from light microscope mounted camera has been revealed as an important need for development of smart processing tools. Obtained images can be used for cell counting and cell viability analysis. In this study, both necessities are investigated as different approaches of solution. Although the commercial automated cell counting systems are available but their high cost limits the broad usage.

This thesis particularly focuses on the preclinical, in vitro experiments in terms of cell monitoring. It directly contributes the cell counting and viability analysis by adding automated method without changing the manual cell examination procedure. In vitro experiments are included all cytotoxic tests for cell culture that are employed from examined cancer type. Before the beginning of tests, the cancer cells are first taken out of the liquid nitrogen and directly thawed into water-bath. Then, these cells are transferred to a culture flask on a culture medium and they are left into an incubator for proliferation.

When the cells are reached to required density and maturity level, they split into the equal portions, such as, control group and test groups. Control group keeps monitoring the casual changes of the cell culture without any external drug. Test groups include cell cultures with the addition of tested drug at various dozes. All portions need to be examined systematically during the tests by experts to estimate cell quality and quantity changes over time (Figure 11). Accepted inspection intervals are 12, 24, 48 and 72 hours.

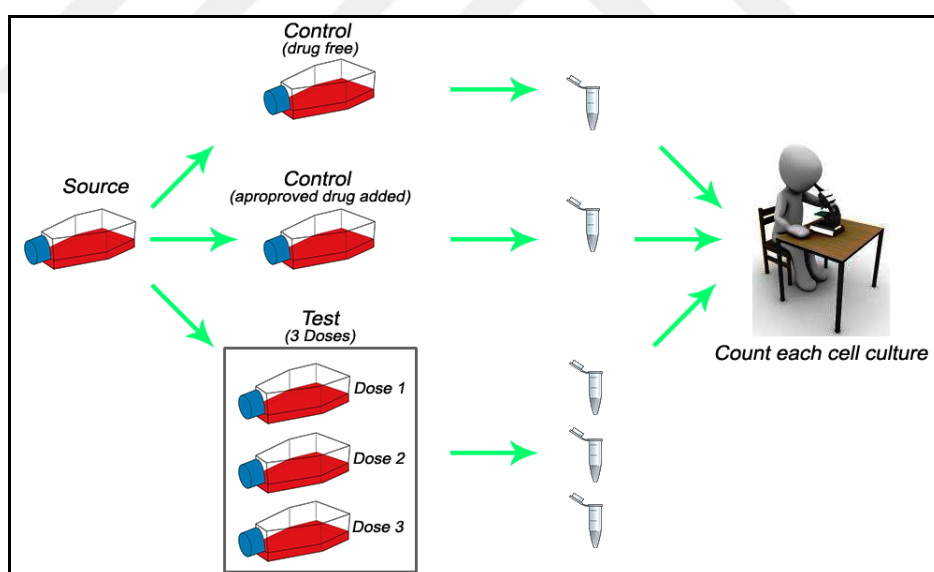


Figure 11. Typical anticancer drug discovery experiment flow

Traditionally, cell counting and cell viability analysis are usually done manually with the help of the microscope and hemocytometer by experts. A variety of false impressions are common in manual counting process causing by human errors about considered cell culture. Examiner's experience and tiredness substantially affects the accuracy throughout the manual observation of cells. The unsteady estimations of

cell density may end up with a biased observation results accordingly. Therefore, an automated cell counting system is inevitably needed to improve accuracy and consistency of the both cell counting and cell viability analysis processes.

Although the gridlines on hemocytometer are critical for manual cell counting, they are big handicaps for image processing based digital analysis. Simple solution is to erase these lines from input images by normalizing the value of background color with the white lines. When this approach is applied to the input images, the white lines are eliminated but the cells on these lines are lost and it makes unreliable the counting result.

The first existing automated solution for cell quantity analysis is flow cytometry [26]. It is a technology that is used to analyze the physical characteristics of cells in a fluid as it passes through laser. It has various disadvantages as follows:

- requires management by a highly trained specialist,
- on-going maintenance by service engineers,
- laser calibration and cleaning for each use.

Additionally, there are end-user automated cell counters [27]. They operate either via electrical impedance or direct imaging. Electrical impedance based systems usually cannot produce the information of alive or dead cell quantity. Imaging based solution has two main disadvantages such as, high investment cost and operational cost.

1.5. Contributions

This study presents an alternative, advantageous and adaptable method for light microscope to be used as automatic cell counter for counting the most known cancer cells. In the study, the method conducted multidisciplinary research areas include; cell biology, computer vision, machine learning and software engineering to reveal the optimum solution.

Additionally, since there is no known data set to be used commonly in the studies of this research field, a novel data set has already created and the dataset has opened to public use for academic research.

The basis of the proposed method is the adaptation of hemocytometer-based manual counting to automated procedure by adding middleware decision software to reduce its shortcomings. By doing this study, we have provided a variety of contributions. The major contributions of the thesis are summarized as follows:

- convert light microscopy into fully automated cell examiner including cell counting and cell viability analysis,
- support toxicology and anticancer drug discovery studies,
- decrease human labor,
- reduce human-based error,
- stabilize the accuracy,
- accelerate the procedure,
- present novel stained and non-stained cancer image datasets of HL60 and K562,
- particularly, proposed method will be adapted to cancer drug discovery researches in Atılım University Biochemistry Research Laboratory.

1.6. Organization

Proposed conversion method splits into two main chores of research stages namely, cell counting (i.e. Stage 1) and cell viability analysis (i.e. Stage 2). At the first stage, the cell location finding pipeline is defined for a given raw hemocytometer image. Second stage includes the automated cell viability analysis by revealing the best classification model. Finally, third stage reveals the whole structure of automated cell analyzer (i.e. Stage 3) in terms of cell location finding and the viability examination.

In Chapter 2, the existing solution approaches and their properties have been inspected by explaining the research methodology. In Chapter 3, the adapted software enquiring policies are explained during the development of model prototype. In Chapter 4, the technical background is revealed related to the computer vision and machine learning. In Chapter 5, the proposed procedures and methodologies have been presented in detail. Chapter 6, the obtained experimental results are given and discussed. In Chapter 7, conclusion and future work are presented.

CHAPTER 2

RELATED WORKS

Before obtaining related publications, it is required a well-defined research and evaluation method that is repeatable, objective and depends on solid research questions. The benefit of following a standardized and comprehensive process is to have an opportunity to develop guidance for evaluation of future alternative method proposals. Also, this avoids the possible misjudgments.

The important data items are extracted as shown in Table 1 from each study to answer. To find the relevant publications, we searched six major academic paper databases [28], namely, IEEE Xplore, ScienceDirect, ACM Digital Library, Google Scholar, Springer, and Wiley. The extracted data was recorded on a tabular form based on their relatedness, recentness and significance.

Table 1. Obtained data for each publication

| Data item | Description |
|-----------|--|
| Title | The title of the paper |
| Year | The year of the paper that was published |
| Author | The full name of all the authors |
| Abstract | The abstract of the paper |
| Keywords | The keywords of the paper |
| Type | Cell counting or Cell viability analysis |

Logical OR and AND are used to connect two or more search terms to find related publications from databases. AND operator requires all search terms to be in each

item. OR operator at least one search term will be in the search list. The following expression is used to find out relevant publications in the databases:

“(cell OR hemocytometer OR light microscope OR automated)
AND (counting OR viability) AND (image processing OR
computer vision OR machine learning OR supervised learning)
OR (HL60 OR K562 OR anticancer OR drug OR toxicology)” (2)

During our research, singular data items are used for the distinction of publications for previous extraction. We have followed the rigorous search strategy to discriminate the related publications from the whole literature which is illustrated in Figure 12.

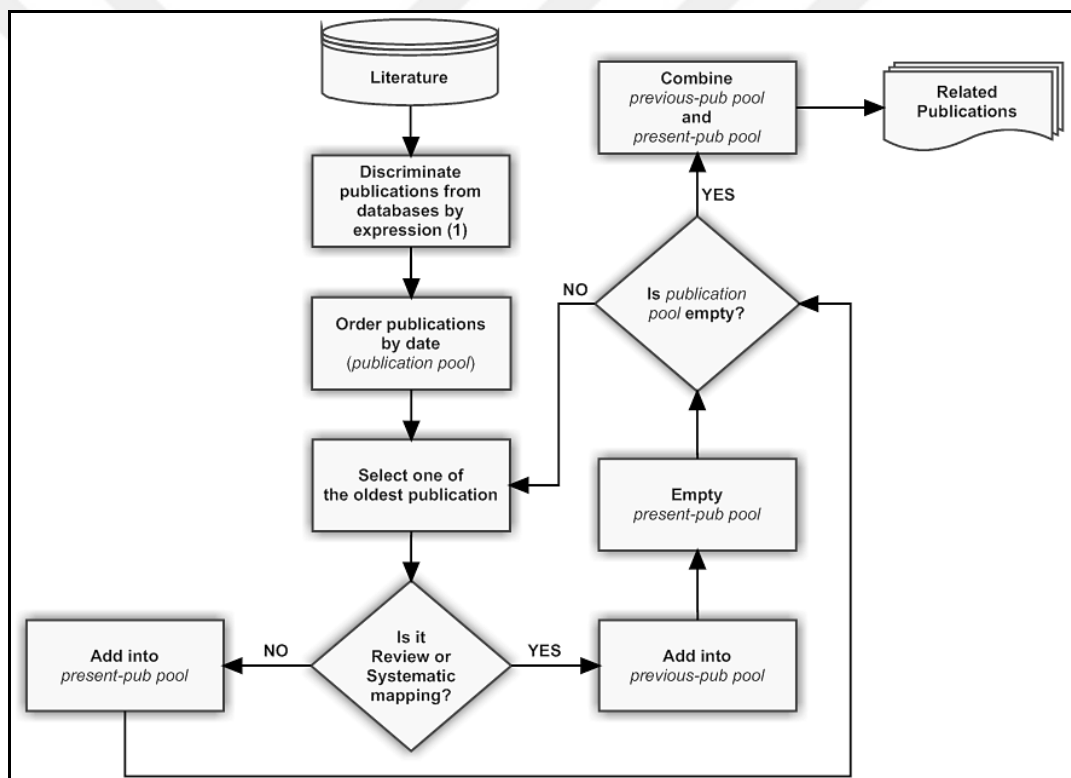


Figure 12. Our preliminary iterative research strategy

We collect a list of publications that discriminated from the literature by using the expression (2). In order to make iterative search, this list is ordered by their publication dates from oldest to newest. Then, we select a paper from the top of the list –i.e. corresponds to the oldest one- and control the fact that the selected publication is a review paper or not. If it is a not a review paper, we insert this

publication into a new list so called “present-pub pool”. Otherwise, we add the publication into another list named “previous-sub pool” and clear the “present-pub pool”. This process continues one-by-one under there is no more paper in the initial publication list. By this way, we iteratively obtain a review paper list “previous-pub pool” and a list of most recent papers that “present-pub pool” has not been reviewed yet. In the end, we categorize the “previous-pub pool” according to their publication dates and we elicit the previously defined information from the papers in “present-pub pool” to answer the research questions.

At the end of the iterative search, all the found relevant publications are examined in full detail as the related works. Related works are investigated in two distinct research topics namely, automated cell counting and automated cell viability analysis.

2.1. Automated Cell Counting

Automated cell counting studies can be grouped under three major categories, namely, cell counting in blood cell, cell (or bacteria) colony counting and hemocytometer based cell counting (Figure 13).

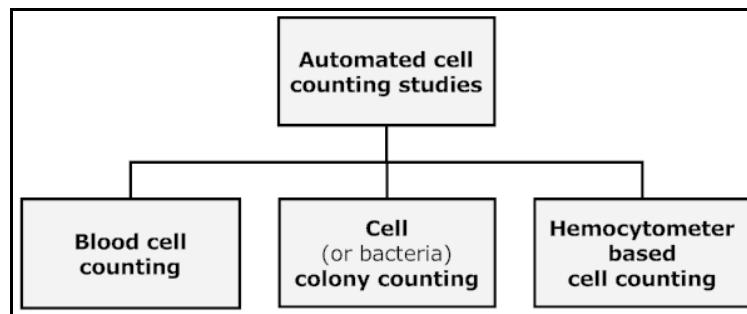


Figure 13. Automated cell counting literature

In the first category, there are numerous numbers of studies have been done for blood cells. Essentially, in these studies [29-31], two common characteristics have been emerged. First, the methods have been adapted blood cell images with the high microscopic magnifications (e.g. 1000x). Second, those studies do not use hemocytometer and the used images have only cells on uniform distributed background which is easy to distinguish.

S. Fabio et al. [32, 33] published two informative papers by surveying the techniques for particularly cell segmentation. Also, R.D. Labati et al. revealed an open access dataset [34] for microscopic images of blood samples namely Acute Lymphoblastic Leukemia (ALL). These publications have turned into well known studies in their research field and have become baseline for many recent studies.

A. Hamouda et al. [35] offered an image based automatic counting system for blood cells. As a result, it was claimed that the decision tree method gives the best result in terms of high sensitivity and accuracy of 97%. There is also more specific investigation to count and distinguish fetal and maternal blood cell types on red blood cell smear (RBC) [36]. They report improved results by approximately 90 times compared to manual reading. Specifically, they claimed undercounted and over-counted result less than 1.7% and 0.9%, accordingly.

The second category, cell colony counting is a fundamental way of gathering information about cell culture which stays at the petri dish or agar plate [37-39]. Researchers have used this information to evaluate side effects of the antibiotics or drug safety etc.

G. L. Masala et al. [40] introduced a new way of automated colony counting method. Initially, they defined a counting area as regions of interest (ROI) automatically and then they applied different filters to enhance the image quality. They analyzed partials using k-nearest neighbors (KNN) and feed forward neural network (FF-NN) as two machine learning algorithms. After all, they compared each result in terms of mean accuracy percentages. They conclude 91% for KNN and 92% for FF-NN.

In another study, Pei-ju Chiang et al. [41] proposed fully automated colony counting system. They designed a special image capture cabinet to take colony images. They also proposed a method to extract colonies from the dish's rim and division of overlapping cells. To evaluate overall system performance, the results were compared with two freely accessible counting systems. Their evaluation showed that the proposed system has accuracy by mean value of absolute percentage error of 3.37%.

The third group of automated cell counting literature is hemocytometer based cell counting. Although there have been many studies in the literature related to cell counting in blood cells and cell colony counting, only a few of them are related with the automated hemocytometer based cell counting.

In the study performed by the Brinda et al. [42, 43] using leukemia cells; the cells are segmented using recursive algorithm. They tested proposed algorithms using conventional hemocytometer's corners and limited number of test images. At the end of these studies numerical results of leukemia cell population are given as the total number of single and cluster cell in an accuracy of %95-%100.

Claudio and Leonilda [44] established a study which is based on the blood samples of three wild animals. In this study, cells are counted by using the captured images at two different focal settings which means that users have to acquire twice the considered sample. They claimed the method found approximately 97% of cells.

There are two distinct recent studies in automated hemocytometer based cell counting literature. Yu-Wei Chen et. al. [45] advises an approach that uses only image processing to count the number of cells in a given image. Corner of hemocytometer has been used as counting area and probability of cell overlaps was not considered. Claimed as the highest hit rate was 100% and the corresponding miss rate was 0%. They reveal their test results obtained by 6 different images.

F. Chobngam et al. [46] proposed a preliminary solution that particularly considers counting of death cell. The method consists of five steps; acquiring, cell extraction from a background, noise reduction, cell counting and output. The correctness of experimental results was in variation from 33% to 97% and 74% to 100%, for death and alive cells counting, correspondingly.

In one newest study Dong Sui et al. [47] concentrate on insect cell counting pipeline using bright field microscopy. They used over focused images to reduce hemocytometer's line domination with respect to cells. The pipeline based on combination of nonlinear filter and sliding band filter called transformed sliding band filter (TSBF). Their concluded average error rate is 2.21% on average, ranging from 0.89% to 3.97%.

In our knowledge there have been no studies found as a comprehensive pipeline for all adverse conditions on hemocytometer based cell counting field like cell shape deformation, image brightness differences and possible impurities caused by cell suspension. Additionally, in the literature there have been no public dataset for HL60 cancer cell that can be used for studies to count the cells based on the hemocytometer.

2.2. Automated Cell Viability Analysis

Previous automated cell viability analysis studies can be divided into three main groups of research areas (Figure 14) regarding the use of image content; namely, Histological, Cytological and Hematological. Each category has host distinct complexity level, depending on the requirements of examination. In the following paragraphs, the related works are summarized by focusing to the most recent studies on each category. Also, during the flow, instead of individual studies, general trends were mentioned and comprehensive review publications are listed which are formed by individual studies in details at the end.

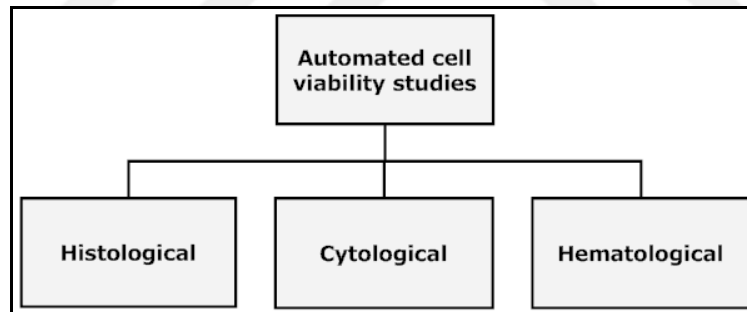


Figure 14. Automated cell viability literature

Histological images [48] include tissue sections which are consisting of ground substance (i.e. extracellular matrix) and cells. First, the tissue sample is removed from the living body by the biopsy procedure [49]. Second, several consecutive sub-processes are applied to thin the sample without harm its content until light can pass through. Finally, a thinned and dyed sample with one of the special stains is examined using microscope by expert. While the automated histological examination, there are different classification techniques adapted to get various

inferences such as, define location of cells [50], determine type of cells [51] or both [52] one after another.

As the second category of related researches, cytological images [53] mainly contain cells and there are various ways to obtain these cells. One manner is isolation of cells directly from tissues [54] with the help of the various separation processes (i.e. primary cells). Also some type of the previously extracted cells from tissues may proliferate in cell culture by creating needed conditions artificially using incubator [55] such as, optimum level of carbon dioxide and temperature.

Another advanced method is based on decomposition of cells from the body fluids [56]. Basically, a drop of liquid sample is spread over a glass slide in a thin layer (i.e. smear). Then, expert examines the smear preparat manually via microscope. Our work is also part of the research field. We used the image data sets of stained HL60 and K562 cancer cell lines that we obtained from light microscope using hemocytometer.

Third group of studies are related to hematological images [57]. The images in this category mostly contain cells same as cytological images. The main difference is that the types of considered cells are only related to the blood cells to inspect for abnormalities in blood sample. Blood normally contains many components in certain rates such as, red blood cells and white blood cells. Each blood element undertakes different tasks. Red blood cells are responsible for transporting oxygen throughout the body. Besides, white blood cells are helping to fight against infections. Abnormalities might be seen in the number or shape disorder of blood cells and it can be indication of a disease [58].

Additionally, there are numerous comprehensive reviews have been presented for each research group by different researchers. Particularly, specific cell-based method benchmarking studies has been presented to describe recent advances in the manner of algorithmic success [59].

Some of the reviews have become prominent to summarize the each research field. Humayun Irshad et al. [60] evaluated major trends for various segmentation, feature

extraction, and classification techniques using histological images. Also, they are outlining all methods in details as a tabular form that is very useful to quick sense.

Christoph S. et al. [61] aims to provide the guidance for the biologists by comparing method of machine learning on microscopy assays. First, they summary basic research areas for cell culture and machine learning studies. Then, they discuss how to optimize data analysis pipeline to classify various cell phenotypes. They have benefited from a lot of previous studies in a chronological order.

M. Saraswat and K.V. Arya [62] have categorized and evaluated recently developed methods for cell segmentation using classification approaches on variety of tissues and blood smear images. Also, they presented possible future research areas and discussed the challenges faced by the pathologists.

J. Rawat et al. [63] provides a review of classification techniques for white blood cells which have been implemented by many researchers. Finally, there are two distinct recent reviews in automated breast cancer detection on cytological and histological images. M.A Aswathy and M. Jagannath [64] discussed a mixture of techniques used for histological image in the perspective of present status and future possibilities.

Throughout our literature investigations, there is no related benchmark study found in which light microscope and hemocytometer based automated viability analysis using HL60 and K562 cancer cell images to define the best classification model was studied.

CHAPTER 3

SOFTWARE ENGINEERING

Software is becoming more indispensable in various areas [65] including, business, military, and health. While software is enabled important functionality, it also requires extra effort to guarantee that quality demands are meeting within the available resources [66]. Obtained information can be used to evaluate the maturity level of software before the release date.

Software engineering is involve [67] development, operation, and maintenance of software product using systematic, disciplined, quantifiable approaches. It's mainly concerned with delivering functional, reliable and efficient software by well-defined scientific principles, methods and procedures. The process of developing a software product using software engineering practice is referred to various approaches. All of these principles can be used with strictly defined methodologies as a package, such as; AGILE [68] or the necessary components can be combined as traditional by depending on the complexity of project. In this thesis, many practices belonging to software engineering are used. Those are requirement analysis, quality checking, software process model definition and algorithmic complexity analysis which are presented in detail below.

3.1. Requirement Analysis

During the software development process, there is often a gap between software developers and the end users who is going to use the software for their needs [69]. This gap often causes the wasted investment to reach the solution because software's capabilities do not meet with the end user's need. Software that does not meet user requirements is not used after a while. Requirements analysis [70] (i.e. requirements

engineering) mainly aims the elicitation of essential user expectations systematically in details.

Requirements are categorized in several ways but they can be summarized under two headings namely, functional and non-functional [71]. The functional requirements describe the behavior of the system in terms of system's functionality. The non-functional requirements describe performance characteristics of the system. Basically, functional requirements state what the system has to do, while, non-functional requirements explain how the system works.

In the life cycle of software development, new requirements can be added, current requirements can change or even can be canceled depending on the feedbacks of users. Requirement analysis work flow has to be flexible during the development. Most of the time non-functional requirements have been ignored in software design. Non-technical features often have a significant place in determining the quality of the software, but they can often be forgotten in software projects.

In this study, a method is introduced to the solution of a problem that is in the field of cell biology. For this reason, technical and non-technical requirements are elicited from experts by several interviews. In addition, feedbacks are received during the development stages from field experts to ensure that the requirements are meet user needs.

3.2. Quality Checking

Software testing notion is a process of executing a software function with the aim of finding the software faults or defects [72]. It intends to make sure that outputted results are as expected using different testing strategy. Software quality checking includes various set of continues sub-process during the project such as, testing. Defect detection and prevention is the one of the crucial sub-task that directly affects overall software quality via testing.

There are two common types of testing [73] namely, black-box and white-box testing. Both of the test strategies can be adapted in the development steps. The proposed method is implemented by using Matlab development environment [74].

This software package is chosen, because it provides an effective platform for matrix operations and has many different toolboxes to support the productivity. We have benefitted its build-in toolboxes and also implemented huge amount of additional script depending on our needs. Hence to overcome the possible software defects (i.e. bugs and errors) we have benefited from both testing strategies.

3.3. Software Process Model

Generally, software development includes various phases performed during the process. Software process model, also known as software life cycle model, is prescriptive model of what should be done from beginning to the end of the development [75]. The main function of the life cycle model is to determine the order of the different phases. Another important function of the life cycle model is to determine the transition criteria between phases. In other words, what the model should describe is what should we do next and how long should we continue to do it for each phase.

Spiral model [76] is an incremental risk-oriented lifecycle model that has four main activities listed: determine objective, identify and resolve risks, development and test, plan the next iteration (Figure 15). Since our project includes three stages, spiral model is chosen as a software process model. The steps suggested by this model are followed at each stage from 1 to 3.

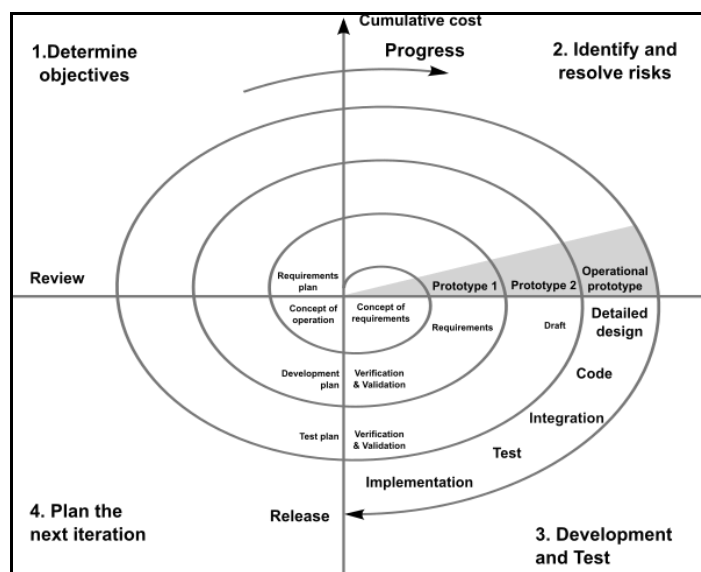


Figure 15. Spiral software process model

A software project goes through these four phases in an iterative way. In the first phase, the requirements gathered. In the second phase, the risk and the alternate solutions identified, and the prototype produced. Software and tests for the software are produced in the development and test phases, which is the third step of the process. Finally, in the fourth phase, the output of the project, so far, is evaluated, and the next iteration is planned. This cycle was repeated at each research stage.

3.4. Algorithmic Complexity

Algorithmic complexity investigates the performance of an algorithm in terms of execution time and used resources [77]. A given algorithm may take different amounts of time on various input sizes depending on its time complexity. Also it uses a range of system resources, such as, disk space, ram, etc. Since, our method runs on ordinary system resources, algorithmic complexity investigations mainly focused on time complexity.

Depending on the processor speed and instruction set, even a huge complex algorithm can be quick if run on small amount of data. This fact leads to inconsistent evaluation results for algorithm efficiency by analyzing execution time in seconds. Hardware independent evaluation process is required to estimate valid complexity characterization for each algorithm according to their runtime performances. Asymptotic notation [78] has been advised to measure time complexity of an algorithm regardless of the hardware variations, including, Big-Omega (i.e. Big-O) notation [79].

Big-O, commonly symbolize with the “O” and indicates the worst case for a given algorithm. Basically, it describes the general duration tendency of an algorithm under the large variety of inputs. It uses behavior of well-known mathematical functions.

Here is a list of Big-O functions that are commonly encountered. They are ordered by better to worse time complexity as follows:

- $O(1)$, an algorithm that will always have constant execution time regardless of the input data size.
- $O(\log n)$, log time.

- $O(n)$, linear time.
- $O(n^2)$, quadratic time.
- $O(n^3)$, cubic time.
- $O(n^c)$, polynomial.

Where; n is size of problem, c is some arbitrary constant.

Basis of our algorithm is sliding window approach. Every possible square sub-images are cropped sequentially to make the decision. The most basic form of our method's singleton can be summarized as nested loop given below.

```

for 1 to X loop1
    for 1 to Y loop2
        Operations
    end loop2
end loop1

```

The outer loop executes X times. Every time the outer loop executes, the inner loop executes Y times. The nested loop execute a total of $X*Y$ times. In our case, X and Y can be assumed as the width and height of an image respectively. In this case the complexity becomes $O(n^2)$. On the contrary, the resultant complexity does not indicate the correct argument.

Proposed algorithm is not taking account whole image. Raw image is filtered before the algorithm begins to reduce unnecessary assessments by using edge density. It leads consideration of only non-empty image windows during sliding. This paradigm was explained in the subsequent sections of the thesis. (Chapter 5.2.3) Numbers of considered image patches characterize the time complexity.

Figure 13 illustrates the plotting of considered number of windows versus required time using whole dataset images on our method. Since each operation take same amount of time, complexity changes linearly depending on number of considered windows. Thus, proposed methods complexity is $O(n)$, where n is the considered number of windows (Figure 16).

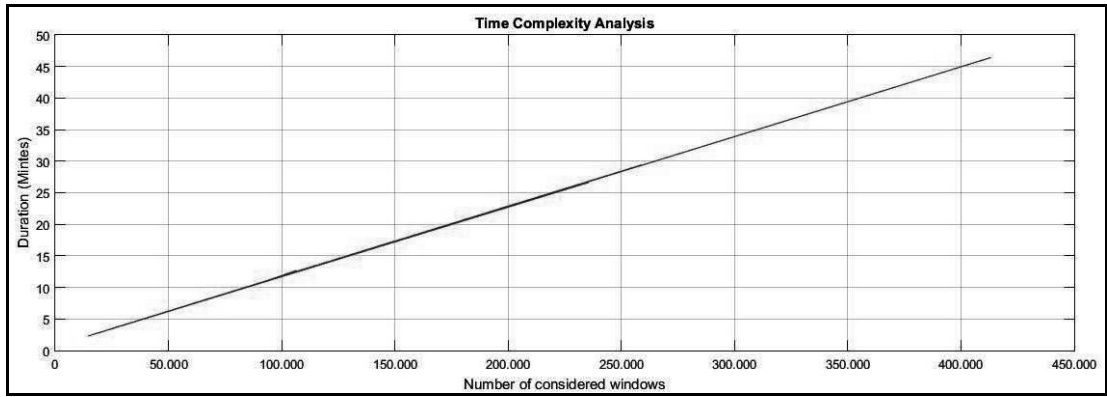


Figure 16. Time complexity analysis (number of windows versus required time)



CHAPTER 4

TECHNICAL METHODOLOGIES

In this section, a number of necessary fundamental concepts will be recalled that are used in the proposed method. Image processing, computer vision and machine learning have become major topics to derivate optimum solutions combining with mathematic and algebraic backgrounds. Actually, these three fields are nested and they cannot neglect one from others. In order to improve the understandability, the underling purposes of these methods will be expressed briefly in the following of the report. Recently, different machine learning based classification approaches and feature extraction methods widen the scope of adaptation on many problems as a decision maker.

4.1. Feature Extractors

In the most cases, the representation of image patterns is the fundamental stage. The assumption is to extract distinctive specification alongside of preserving robustness against diversity as much as possible. This representation phase is generally called as feature extraction [80]. After representing of image with suitable features (i.e metrics), machine learning is utilized for distinguishing defects into meaningful classes according to their shared properties as classification model. This classification can be made using human labeled data namely, supervised learning [81]. The robustness of representation and the success of classification are deeply interrelated with each other.

Feature extraction and machine learning have become major topics to derivate optimum solutions combining with mathematic and algebraic backgrounds. Actually, these two fields are nested and they cannot neglect one from other. In order to

improve the understandability, the underlying purposes of these methods will be expressed in the following parts of the study. In this study, we employ three promising feature extractors, namely, local Binary Pattern (LBP), Local Phase Quantization (LPQ), and Histogram Oriented Gradients (HOG).

4.1.1. Local Binary Patterns (LBP)

The LBP initially presented by Ojala et al. [82] to form labels based on the image pixels by considering the 3 x 3 neighborhood of each pixel with the center value thresholding (Figure 17). The essential idea is to describe image by using only local features of a textural variance. LBP image descriptor labels the concerned pixels as a binary number depending on the gray scale variance of surrounding neighbor pixels by using center pixel value as a threshold. If the intensity of the center pixel is greater or equal to the neighbor, then it is denoted by 1 and otherwise it is denoted by 0.

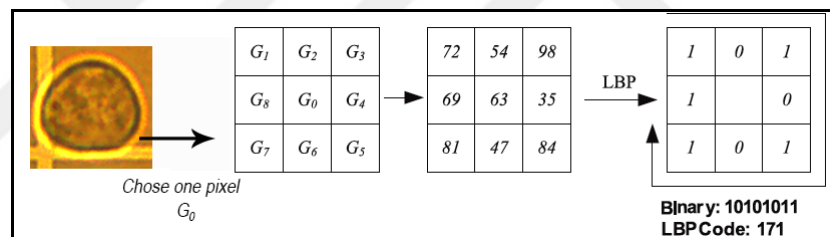


Figure 17. Example of LBP using 3x3 window

It was extended by various modifications in the following years to increase the applicability [83] such as; circular neighborhood (Figure 18) extension which allows any radius and number of pixels in the neighborhood as explained in (3).

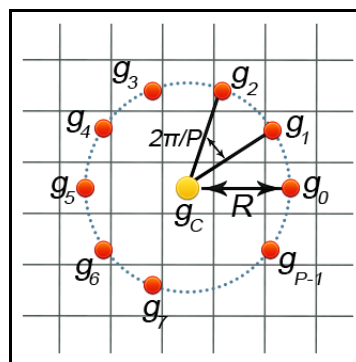


Figure 18. LBP circular neighborhood

$$\text{LBP}_{P,R} = \sum_{p=0}^{P-1} s(g_p - g_c) 2^p, s(x) = \begin{cases} 1, x \geq 0 \\ 0, x < 0 \end{cases} \quad (3)$$

Where,

- g_c : the gray value of the center pixel,
- g_p : the value of its neighbors,
- P : total number of involved neighbors,
- R : the radius of the neighborhood,

The LBP has become a popular approach for texture analysis and object recognition because of its discriminative power and computational simplicity [84]. The most important property of the LBP is its robustness to illumination changes.

4.1.2. Local Phase Quantization (LPQ)

LPQ was originally proposed by Ojansivu and Heikkil [85]. It is widely used for blur invariant texture classification as a feature extractor. The phase information can be used to be a blur invariant property. Also, there are a few studies [86]; LPQ shows better performance for the images that are not blurred rather than other feature extractors such as LBP.

In current LPQ algorithm, first, image is transformed from spatial domain to frequency domain. Second, the local phase information is computed using two well known approaches, namely a short-term Fourier transform (STFT) and Gaussian derivative quadrature filter [87]. The phases of the four low-frequency coefficients are decorrelated and quantized in an eight dimensional space [88]. A histogram of the whole image is created and used as a feature. Generation of histograms is similar to the LBP method.

4.1.3. Histogram Oriented Gradients

Originally, the HOG was proposed by Triggs to use in pedestrian recognition systems [89]. Following the outer performance for human detection, it has attracted

considerable interest from many researchers and is adapted to several object recognition problems as a feature descriptor [90].

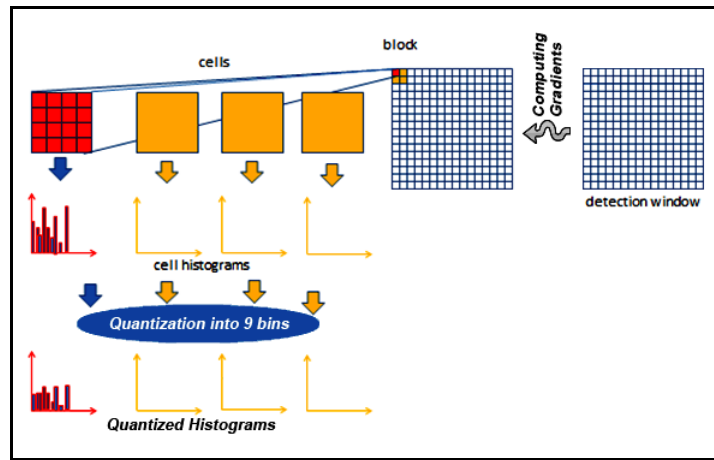


Figure 19. The flow of HOG

HOG method defines the image as a group of local histograms in terms of oriented gradients (Figure 19). First, image gradient is calculated using the gray level image and divided into equal blocks in both vertical and horizontal directions and each block is divided by small identical regions, called cells. Block and cell sizes may vary depending on the problem. Blocks overlap with each other at predefined ratio, so that the same cell may be in more than one block. Second, the gradients are computed per pixel to get orientation and magnitude for the edges. Third, histograms are built for all the cells using unsigned orientations in a discrete orientation bins from 0 to 180 by quantizing the gradient orientations into 9 bins. Additionally, contrast normalization can be applied as an arbitrary step, since several images may have different contrast values. Finally, cell histograms are concatenated including each block as HOG descriptors. It consists of all the cell histograms for each block.

4.2. Classifiers

Classification is a subfield of machine learning that is concerned with finding requested patterns arises in given image. Mainly, supervised learning approaches [91] can be divided into two major fragments, training and prediction (i.e. testing) stages. In training stage, classifier strives to learn optimum distinctive characteristics from unstructured data with data's label information. Then, in prediction stage, label of a random sample is predicted using this pre-generated model. Unfortunately, even

though there is a mathematical/statistical coherence among these data for each category, they are not linearly separable [92] in most of the cases. For this reason, such method needs to estimate optimum separation boundaries for categories by adjusting tradeoffs between true and false decisions. However, in order to construct working model for further predictions, there should be immense number of labeled data and, as expected, this collecting and labeling of data is not simple. The classification approaches used in this study are summarized in the following subsections.

4.2.1. K-Nearest Neighbor (KNN)

KNN can be adapted for classification and regression estimation problems [93]. However, it is relatively more widely used in classification. KNN classification approach is a very straightforward, yet powerful method for the many of the classification cases [94]. The key idea is that related samples belong to similar classes. Thus, before the estimation, certain numbers of the nearest neighbors investigate and distribution of total numbers obtains to assign a class type to the incoming unknown input. It stores all available cases into feature space and classifies new instance by a majority vote of its k neighbors regardless their distance which by default is the Euclidean distance.

The number of the nearest neighbors, k , should be odd in order to prevent ties while estimating total numbers for each class. Additionally, selection of k effects on how well the data can be utilized to generalize the results of the KNN algorithm. A large k values help reduction of the variance due to the noisy data. On the other hand, this might cause ignorance of the smaller patterns which may have useful information. One of the major weaknesses of KNN is that the classifier needs all available data while making decision to new instance. This may cause to negative side effects such as high complexity in researching, if the training data set is large.

Figure 20 illustrates an example of KNN for two classes. Let class A is a finite set of green triangles and B is a finite set of red squares in two dimensional feature space. Different neighboring configurations can be evaluated to decide the unknown instance; it is represented as a blue star.

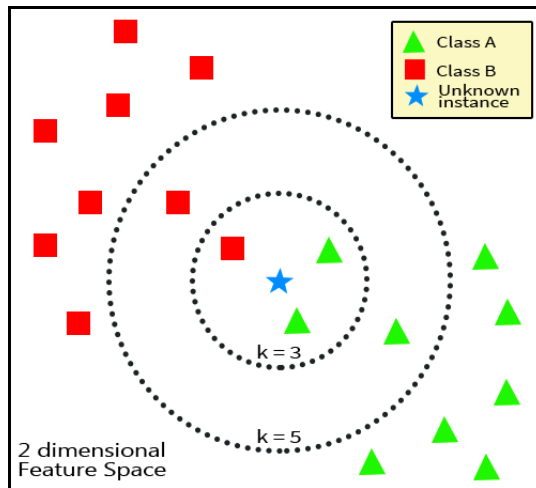


Figure 20. Example of KNN in two dimensional (2D) space

4.2.2. Support Vector Machines (SVM)

SVM was introduced by Vapnik [95] in 1995 for classification and regression problems. It is applied in many different classification problems [96] and produced satisfying results. It continues to be widely used today as one of the famous classifier [97]. It becomes the effective and relatively less complex popular classification method. SVM determines the best possible strength line that maximizes the distance between the different classes (Figure 21).

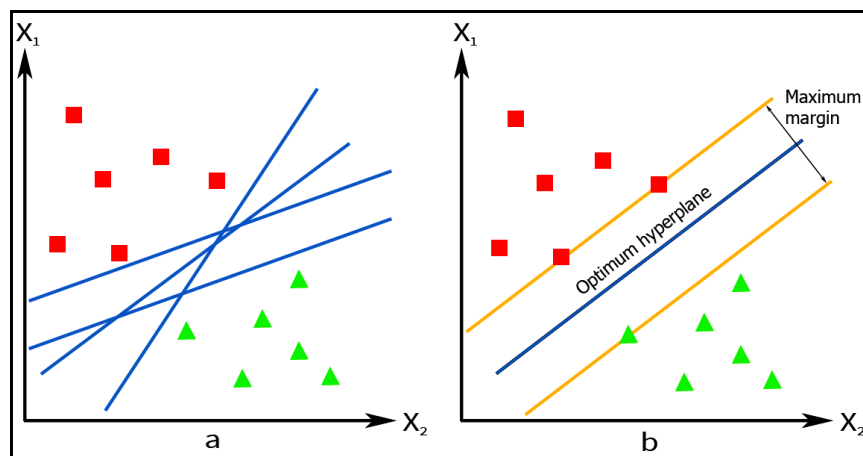


Figure 21. a) Possible solutions for SVM b) the best possible strength line

In other words, it estimates the largest gap (i.e. margin) in terms of distance between two sets of data points as distinct classes and gives a better chance of new data being classified correctly. The determination is accomplished by quadratic programming [98] based optimization to find maximal margin separation between classes. SVM is

basically a binary (i.e. two-class) classifier which considers a binary classification problem by positive and negative class instances. Technically, SVM may extend the binary to the multi-class classification but this type of extension was not needed in this study and it is not deal with in this study.

4.2.2.1. Data Separability

In the classification problems in terms of distribution of the data, there are two distinguish cases:

- data might be consist of linearly separable classes,
- data might be consist of non-linearly separable classes,

Addressed cases apply to binary datasets which is consisting of positive and negative instances. Linearly separable data refers to the existence of a line which separates the two sets of classes in two dimensions (Figure 22). The line splits two classes such that all points of the first and the second class are entirely stay belonging class sides. Similarly, in three dimensions it means that there is a plane and in higher dimensions, there must be a hyperplane which completely separates two classes. On the other hand, non-linearly separable data require a bit of complex shape than line to separate the two classes properly. In other words data can be separable but cannot separate using a straight line to split the two classes completely. The best-known example in this regard is the XOR problem.

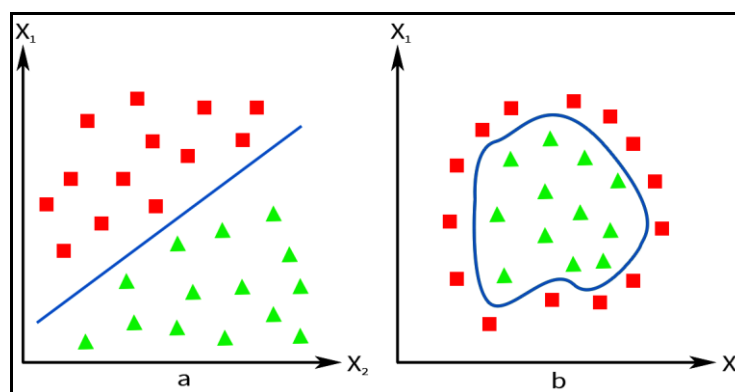


Figure 22. a) linearly separable data b) non-linearly separable data

4.2.2.2. Kernel Trick

Since, SVM can separate properly only if the data is linearly-separable, it will be more accurate to handle the subject under two different cases; hard margin and soft margin.

SVM's linearly separable data necessity appears to limit its capabilities to apply all classification problems. The limitation can be overcome by an extension called kernel trick [99]. It gives a chance to apply SVM efficiently over non-linear problems by transforming data to a new representational space based on the kernel function (Figure 23) and then apply classification techniques.

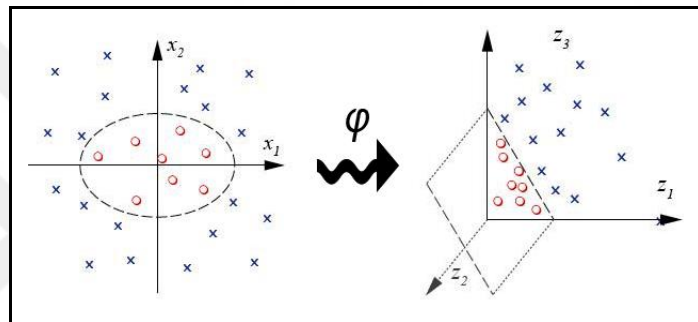


Figure 23. SVM kernel trick

Kernel trick actually allows many linear methods to be used for non-linear problems by virtually adding additional dimensions to make a non-linear problem linearly separable. Linear classification is performed in the higher dimensional space with kernels so that it may produce non-linear classification in the original space. The most commonly used kernels are polynomial and radial basis functions (rbf). This flexibility of SVM does come at the cost of computation. The Gaussian rbf kernel is one of the most often used kernels in practice.

4.2.3. Random Forests (RF)

Decision Tree [100] approach is a fairly straightforward way of solution to various classification and regression problems. It has been around for decades and recent variations such as, random forest [101] are the most powerful and promising classification techniques. The idea depends on a model creation that predicts the class category of an input variable by learning simple decision rules inferred from the

data. Binary decision trees are also very similar to binary trees. It is tried to obtain a more homogenous tree structure. The fundamental difference is that it allows only two nodes that formed from the root node. Additionally, leaf nodes of the tree contain an output that is used to make a prediction (Figure 24).

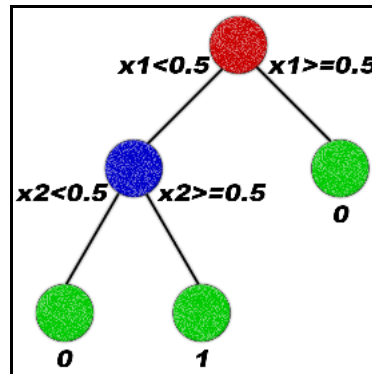


Figure 24. The tree has three types of node; root node (red), internal node (blue), leaf or terminal node (green)

Today, decision tree algorithm also mentioned by intuitive name CART which stands for Classification And Regression Trees. The CART represented by binary tree and the tree can be accumulate in file as a graph or a set of rules.

The main goal of building the maximum tree is to obtain the most pure, best partition condition. Two algorithms are used for this [102]. These are the GINI and Twoing algorithms. If we look at the GINI algorithm first, the goal is to get the largest set of data in each step. Thus, the best splitting situation will be achieved. Also, after the division, the part that we are not interested in is isolated.

The Twoing algorithm provides a more balanced structure than the GINI. The reason for this is that each time it tries to contain 50% of the parent and child nodes. Therefore, there will be a slowdown according to GINI.

The second step is to determine the depth of the tree. For this, let n be the minimum number of records that a node will have. If this value is less than user defined value n , the algorithm will stop working. This value is usually chosen up to 10% of the sample data set. It does not need to be described in a mathematical form. The structure can distinguish important and insignificant data. It has the advantage of working with noisy feed. It does not require any acceptance.

Binary decision tree has advantage in terms of speed but is infamously bad at generalization while using for classification, regression, or clustering. A Random Forest is formed by the combination of several decision trees to boost generalization ability of a single tree. Each decision tree includes random subsets of the data. This led to capture different trends in the data by different tree. Based on the idea, each tree has a "vote" during the classification and predictions based on the majority of the votes (Figure 25).

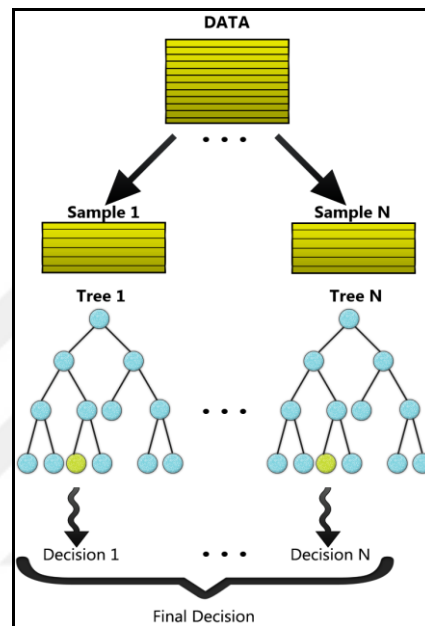


Figure 25. Random forest

4.3. Cross Validation

All possible combinations of the feature extractors and classification approaches (i.e. model) should be investigated, since there is no universal rule to maximize the classification success for all classification problems [103]. Model evaluation concept is preliminary aims the assessing of the best settings of classifier to maximize the prediction accuracy. Besides, the features used as input also have affects on the classifiers harmony. All the feature extractors and classification approaches have one or more tuning parameters those have direct effects on the overall performance.

Cross validation [104] is the systematic way of deciding the most compatible model by trying the different possibilities of the parameters. There is various cross validation techniques to define the optimal parameter(s) for a given classification

problem, namely, hold out, k-fold, leave one out. K-fold [105] cross validation is the most common one in terms of speed and resource requirements.

k-fold cross validation consists of several consecutive steps as follows:

- Select a number of k to partition the data set.
- Partitions the data into k disjoint, equally sized folds, such as $F_1, F_2, \dots, F_{(k-1)}, F_k$
- For each fold ($i = 1, 2, \dots, k-1, k$):
 - leave out one of the partitions as a test set and the other k-1 partitions as a train set each time.
 - train a model using the train set by changing either feature extraction or classification parameter. ($y_i: X \rightarrow C$, where X is feature space and C is set of classes $\{1, -1\}$ on the basis of D/D_i and c is target to be learned)
 - Assesses model performance using test set

$$\text{Err}(y_i, D_i) = \frac{|\{(x, c(x)) \in D_i : y_i \neq c(x)\}|}{D_i} \quad (4)$$

- Calculates the average classification error (i.e. misclassification rate) over all folds.

$$\text{Err}_{cv}(y, D) = \frac{1}{k} \sum_{i=1}^k \text{Err}(y_i, D_i) \quad (5)$$

4.4. Sliding Window

Basically, sliding window approach [106] has certain sized imaginary window (bounding box) and it slides across the input image by predefined step size. Each and every step of sliding, sub-images are cropped from the input image as the predefined dimensions. If we consider the image as a large matrix, sliding window approach can be assumed as the entire process of division operation that is the large matrix into smaller sub matrices (Figure 26).

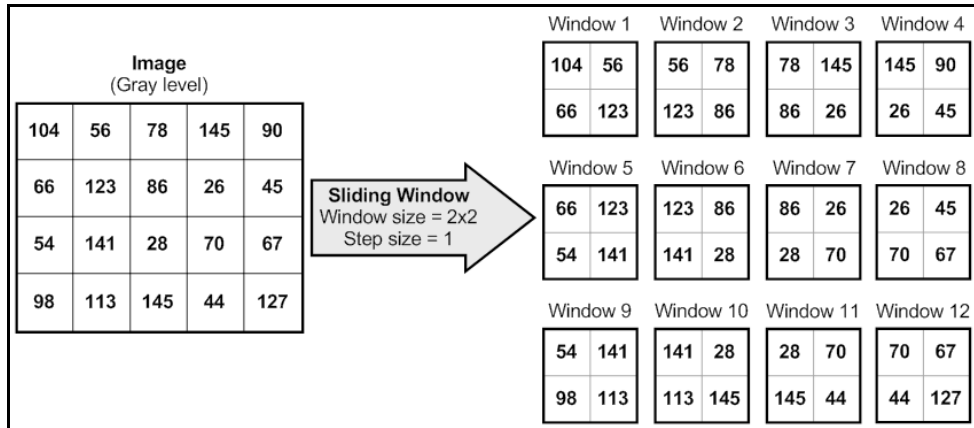


Figure 26. Sliding window

4.5. Bounding Box Collision

A bounding box (i.e. bounding rectangle) is used to describe a convex area and lies at the heart of the collision detection concept [107]. Frequently, it is defined in the format $[x\ y\ width\ height]$, where x and y correspond to the upper left corner. Bounding boxes lie at the heart of the collision detection. Bounding box collision refers to the computation process of detecting the intersection between two or more bounding boxes. Additionally, if the collided area is larger than 0, then overlap ratio must calculate to evaluate the level of collusion. There are two fundamental ratio types, namely, union and minimum.

Both ratio types are formulated as

$$\text{Union type ratio} = \frac{\text{area}(A \cap B)}{\text{area}(A \cup B)} \quad (6)$$

$$\text{Min type ratio} = \frac{\text{area}(A \cap B)}{\min(\text{area}(A), \text{area}(B))} \quad (7)$$

Union type ratio is calculated as the intersection area between bounding box A and bounding box B, divided by the union area of the two (6). Besides, min type ratio is computed as the area of intersection between bounding box A and bounding box B, divided by the minimum area of the two bounding boxes (7).

CHAPTER 5

PROPOSED METHOD

Proposed conversion method splits into two main chores of research stages namely, cell counting (i.e. Stage 1) and cell viability analysis (i.e. Stage 2). At the first stage, the cell location finding pipeline is defined for a given raw hemocytometer image. Second stage includes the automated cell viability analysis by revealing the best classification model. Finally, third stage reveals the whole structure of automated cell analyzer (i.e. Stage 3) in terms of cell location finding and the viability examination.

To the best of our knowledge, there is no publicly available hemocytometer image dataset that can be used for cell counting and cell viability studies. First, we acquire two distinct novel data sets as baselines namely, HL60_HEM40x_CC and HL60_K512_HEM40X_CV that are publicly available for further academic researches. Both datasets are collected at Atılım University Cell Biology laboratory [108], Turkey in multiple sessions.

5.1. Acquired Image Datasets

Cells can be stored at a very low temperature in freezer (i.e.-86°C) to be used in further researches. We obtained frozen cells stored previously. Frozen stock HL60 [109] and K562 [110] cells were carefully taken out of the freezer and thawed in a water-bath. Then the cells were rested to proliferation in an incubator at 37°C with 5% CO₂. The both cells are a kind of leukemia. Since, the HL60 and K562 cell lines provide a continuous source of human cancer cells for drug development studies; they are widely used in cell culture laboratories.

5.1.1. HL60_HEM40x_CC

In this study, we propose a baseline dataset referred to as HL60_HEM40x_CC for further research studies to vision based automated cell counting by hemocytometer. This dataset contains unstained Human Promyelocytic Leukemia (HL60) cancer cell images with magnification factor 40x by hemocytometer (HEM40X) for cell counting (CC). The further specification details of the cell counting dataset are reported in the following sections.

5.1.1.1. Image Datasets

Images are acquired from Motic B3-Series 2.0 Megapixels Moticam 2000 CCD camera microscope by setting the magnification to 40x. Also, the dataset contains 468 RGB (Red-Green-Blue) images in 1200x1600 pixel resolution. We divided the dataset into two subsets as Set 1 and Set 2 on purpose of enabling to use each set in either training or testing stage of a proposed method one at a time.

The dataset contains compelling samples which simulate realistic conditions. Particularly, imperfectly visualization, cell shape deformations, varying lighting, cluttered cells and impurity of cell suspension are some of the artifact types that can be observed in the dataset. Figure 27 illustrates some of the cell samples from the dataset.

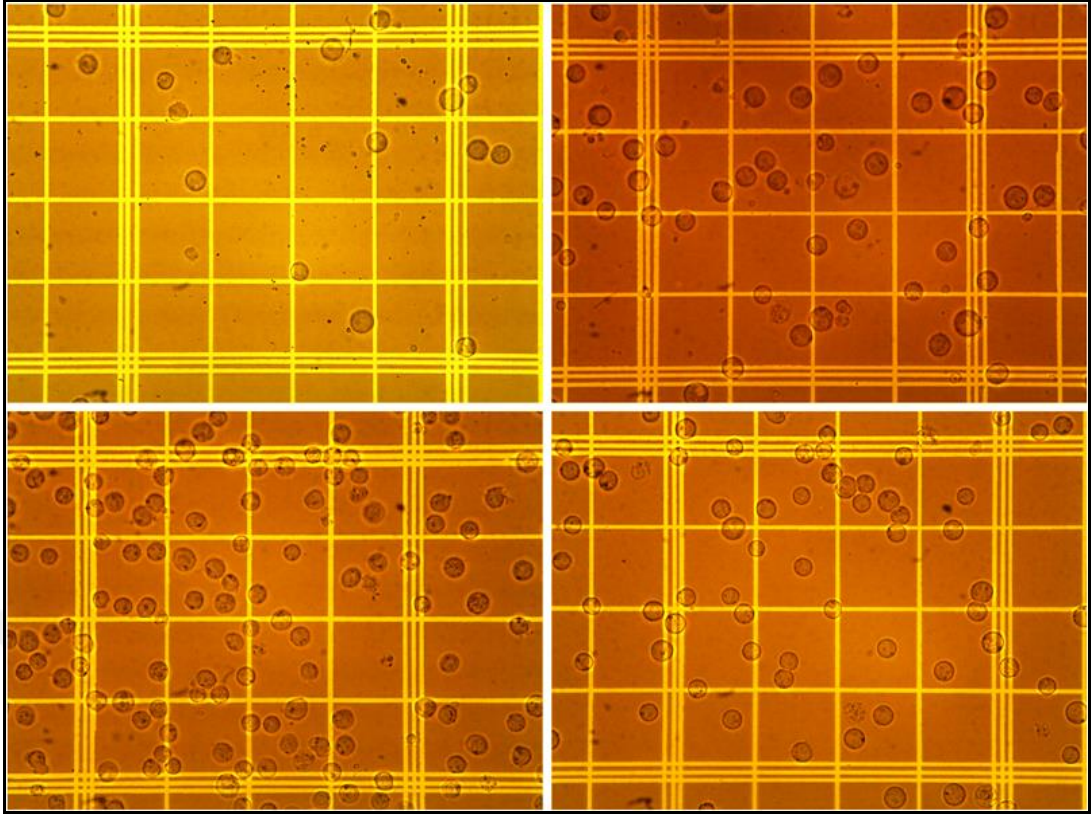


Figure 27. Randomly chosen sample images from our novel dataset those have possible adverse conditions

5.1.1.2. Ground Truth Locations Data

Cell coordinates for each image are annotated by two different experts and the fundamental statistics of the sets are summarized on Table 2. Experts mark all cell locations as Positive and non-cell locations as Negative samples. The collected ground truth annotations for each image are stored in Comma Separated Values (CSV) file format. The coordinate annotations are in bounding box form where x , y , width and height indicate the coordinate of upper-left of the bounding box and its wideness in two axes respectively.

Table 2. Number of annotated HL60 cells for cell location finding (stage 1)

| Labels | Number of cells | |
|----------|-----------------|-------|
| | Set 1 | Set 2 |
| Positive | 2621 | 4269 |
| Negative | 3548 | 4583 |

5.1.1.3. Region of Interest (ROI) Boundary Location Data

To avoid the confusion in counting chamber, the region of interest (ROI) on an image is also provided in the dataset which is also labeled by experts and it has similar file format as in the file that holds the coordinate information. Each file has four rows which define the top, bottom, right, and, left boundaries of ROI, sequentially.

An example is given in Figure 28. Left is considered sample image from our proposed dataset with corresponding ground truth annotations as matrix form. Cell locations are marked by green bounding boxes and four ROI boundary location data drawn by blue bounding boxes. The inside of area covered by these four squares is called the ROI.

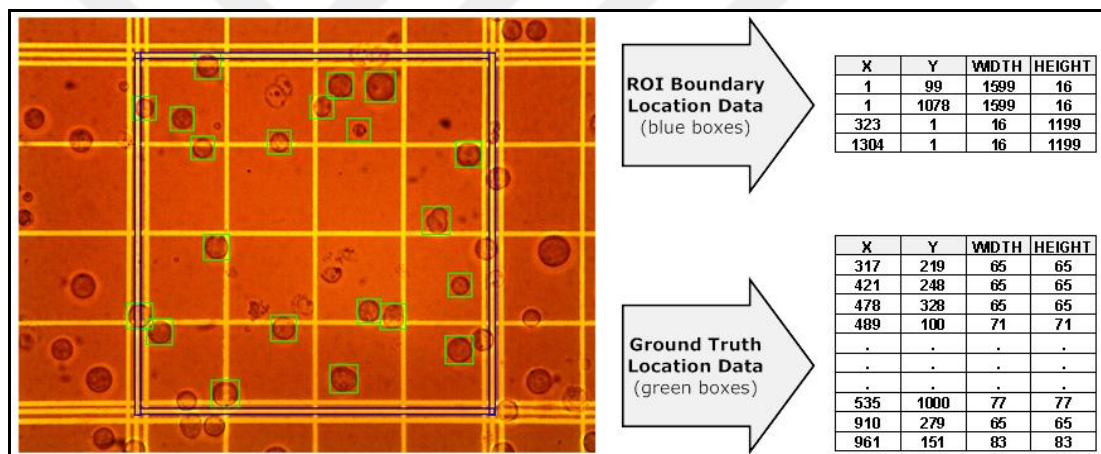


Figure 28. A sample image from the dataset with corresponding ground truth annotations by experts. Cell locations (green), ROI boundary location data (blue).

5.1.2. HL60_K512_HEM40X_CV

The dataset consist of the two classes namely, alive and dead for viable and non-viable cells, respectively. First, we acquired images using a charge-coupled device (CCD) camera which is fitted on a light microscope. Second, the cells in the images were annotated by experts depending on our annotation strategy which is explained in following sub-chapter. Finally, using the annotations, cell patch images are obtained from raw images. The patch image sizes vary between 52x52 to 142x142 pixel dimensions. We named this dataset as HL60_K512_HEM40X_CV: where

HL60 and K562 obviously indicate cancer cell types, HEM40X indicates the used magnification of the microscope is 40x by hemocytometer, CV stands for ‘Cell Viability’ that means cells are stained with the trypan blue dye to cell viability analyzes. The dataset is publicly available to nonprofit usage at biochem.atilim.edu.tr/datasets/. The count of patch images for both HL60 and K562 cell sets are given in Table 3.

Table 3. Number of annotated HL60 and K562 cell images for cell viability (stage 2) and overall method (stage3)

| Class | Cell Types | |
|-------|------------|------|
| | HL60 | K562 |
| Alive | 2738 | 1052 |
| Dead | 2415 | 1071 |

Obtained images include perfectly and imperfectly visualized images. Images have all the possible variety of adverse conditions such as; deformed cell shape, images with different brightness, single cell image with unequal brightness, images having clumped cells and impurities in cell suspension. The image under investigation having any of these unwanted situations makes the automated cell viability analysis harder.

5.1.2.1. Annotation Strategy

The majority of the images obtained were collected during a drug development study in different sessions. After the preliminary image repository was created, images selected from the repository to consider in this study. The total numbers of considered images are 522 and 392 for HL60 and K562 respectively. While making the selection, it was emphasized that there are no cases to make the process of manual counting impossible.

Preferred image has to be as follows:

- There has to be sufficient numbers of cells,
- The absence of dye clusters and medium based particles in large scale,
- The nonexistence of clumped cells,

- The focal setting of microscope must be in a acceptable boundaries,
- The counting field or ROI has to be seen as one-piece.

We have followed the rigorous annotation strategy to discriminate the related cells from the raw images which is illustrated in Figure 29. The images taken into consideration were passed through a three-phase annotation process. On each phase images has filtered by different filters and then annotated by expert as alive or dead. On this count, the expert could evaluate and decide by three different forms of the same image. Additionally, we aimed to minimize the effects of expert cognitive attention changes due to external factors.

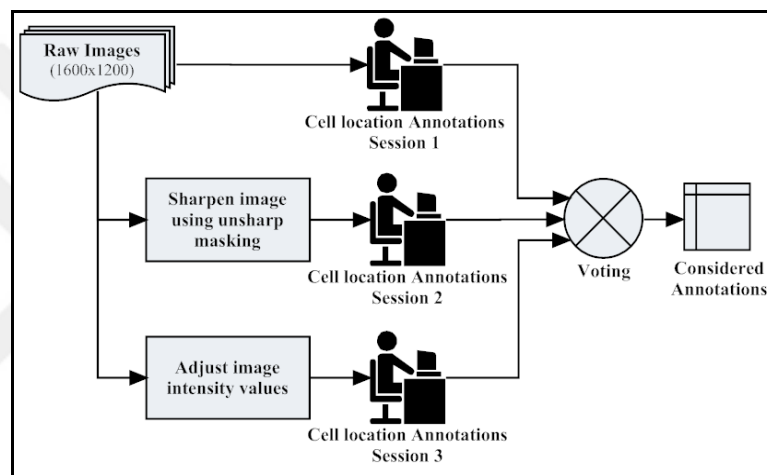


Figure 29. Image annotation strategy

5.2. STAGE 1: Cell Location Finding Pipeline

In this stage, we present a cell location finding and counting pipeline for light microscope images based on hemocytometer that can be easily adapted for various cell types. The proposed method is robust to adverse image artifacts and cell culture conditions such as, cell shape deformations, different lightning conditions and brightness differences of images.

Our method is based on vision-based cell location classification. For this purpose, after search space reduction and visual quality improvement steps, we extract all possible cell candidates from an image using a sliding window scheme. Then, we obtain high confident cell locations using a cell pattern model learned from a training set.

Proposed system might be split into five consecutive steps as shown in Figure 30, so, this section is divided into five consecutive steps to ease the understandability of the proposed method.

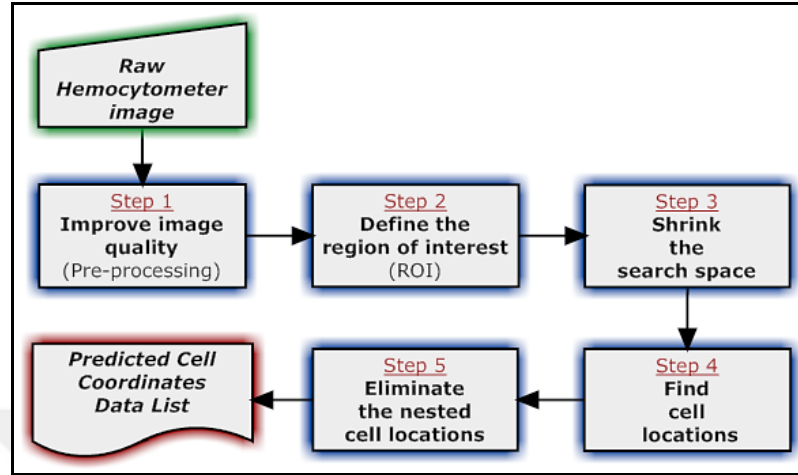


Figure 30. Cell counting pipeline

5.2.1. Improve Image Quality

Basically, image processing (i.e. Digital Image Processing) seem as the union of concepts those are covered by signal processing field on discrete domain such as, image filtering. It is frequently selected as a preprocessing step to enhance the performance of the offered pipeline. The success rate of a proposed method highly depends on the image quality and it is important to keep image qualities at an optimum level to avoid unwanted artifacts such as low contrast level. At this step, one conventional approach is to apply a contrast enhancement to raw input image. Therefore, raw RGB input image is converted to gray level image in advance by formulating a weighted sum of the R, G, and B components as:

$$\text{Graylevel} = 0.2989 \times R + 0.5870 \times G + 0.1140 \times B \quad (8)$$

In the enhancement step, pixel intensities are mapped to new values by saturating 1% of the lowest and highest intensities of an input data [111]. Raw input images become more applicable for further image analysis. Additionally, this enhancement procedure is applied to all of the training and the testing data.

5.2.2. Defining the ROI

In hemocytometer based counting, there is a rule that needs to be applied to avoid double-counting. This rule imposes that cells that touch the middle of the triple lines on the left and the top of the regions should be counted in the chamber. Also the ones that lie on the right and the bottom of the regions should not be counted. Therefore, this counting region for an image should be determined, before going any further step.

This step includes estimation process of ROI using defined ROI boundary locations which is marked by experts. However this stage might be automated for future studies. One important note is that the determination of search region induces a significantly reduction in computation costs for upcoming steps. ROI boundary locations are deployed with the dataset.

5.2.3. Reducing Search Space

Sliding window approach takes too much time to apply whole input image because it produces a large set of candidate sub-images. Additionally, most of the input images include a fewer number of cells than non-cell (i.e. non-textured) regions. Elimination of empty areas will reduce the search space thus the approach becomes more efficient in terms of the processing time. Also, this improves the precision rates of classifier for non-cell regions.

Edge detection and sliding window approaches are used together to reduce the cell search space. Before finding cell locations, edge detection is initially computed for whole image to define the possible cell location that has to consider. Canny edge detector [112] is applied to each cropped sub-image and we measure the edge density of an image. If this density value is greater than a predefined threshold, our approach considers this sub image as a possible cell location; otherwise it assesses as empty and removes from the target list.

Empirically, we tune some of the parameters that are used in this process. First, we set the optimum window size and the step size as 50x50 and 5 respectively. Second, canny edge detector has three parameters, namely, low threshold, high threshold and

sigma. Low threshold and high threshold are set to 0.020 and 0.055 while sigma parameter is assigned to 1.

5.2.4. Finding Cell Locations

After reducing the search space, the remaining sub-images might still contain non-cell parts. To eliminate these parts and obtain the total cell counts, we should estimate true cell locations by using supervised classification and visual feature methods. The flow chart for cell location finding is summarized in Figure 31.

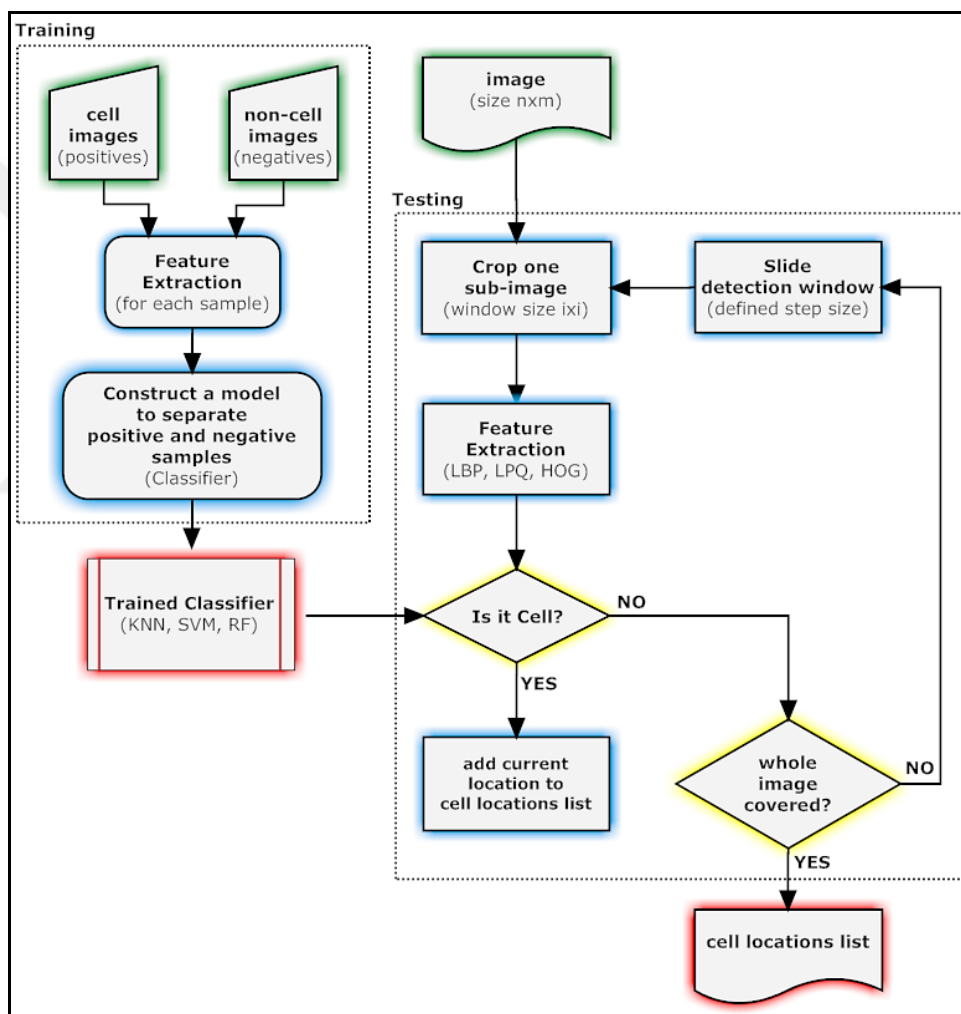


Figure 31. The flow chart for cell location finding

We can separate the estimation of cell location stage into two steps as training and testing. In the training step, a large volume of fixed sized cell and non-cell examples are depicted with different visual feature models and a classifier is trained with these samples. This step generates an optimum visual pattern model for each classification

and feature combination. The important note is that this model is computed once and stored for the testing stage.

In the testing step, our approach accepts all of the sub-images coming from the sliding windows and returns probabilistic decisions as posterior probability (i.e. score) for possible cell locations using the model in the training step. Finally, the detected cell locations are stored in a list with their confidence scores to obtain final locations.

5.2.5. Elimination of the Nested Cell Locations

In the final step, nested cell locations are eliminated from the list. The main purpose of this step is to avoid getting multiple bounding boxes for the same cell. In the previous step, we expect that the classification methods produce higher probabilistic confidences. But most of the time they offer more than one possible locations for one cell location. For this reason, selecting the most suitable response from a large number of outcomes requires an additional strategy. Non-maximal suppression [113] (NMS) is widely used as a post-processing technique in object recognition.

It chooses the best likelihood out of overlapped bounding boxes regarding to their scores. NMS algorithm is an iterative process and it requires parameters: three bounding boxes list, score list and definition of collusion information. Basically, it starts by sorting the locations using their scores in the descending order. Then, each iteration, it selects a random bounding box and compares with the windows that are collided with the bounding box by suppressing the scores. This process repeats until no more collided window remains. The type of the collusion and the threshold are set as Min type ratio with 0.25.

Figure 32 represents an example to explain whole cell location finding pipeline.

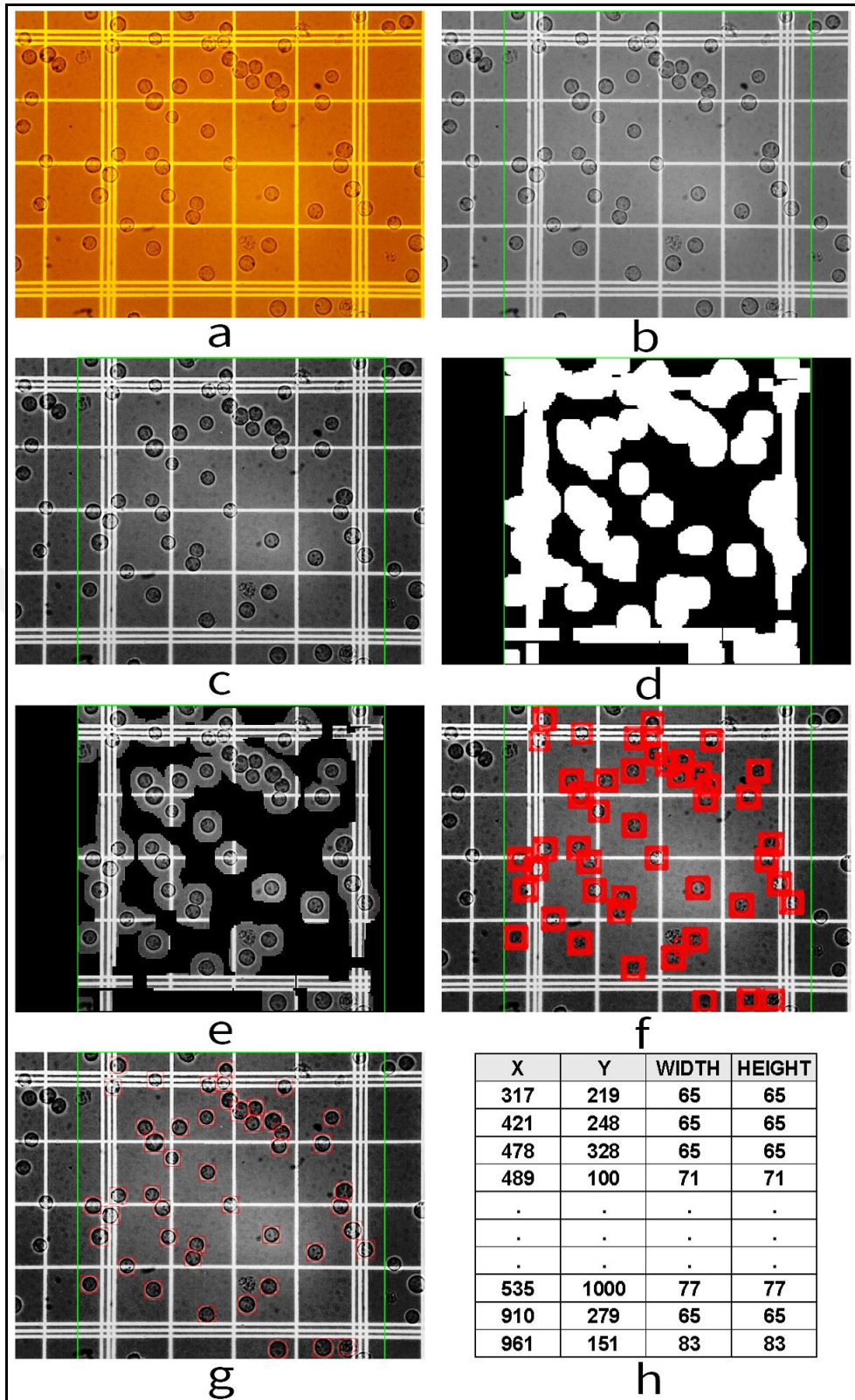


Figure 32. Example of cell location finding pipeline a) Input image b) defining the considered area (green square) c) contrast enhancement d) decide the possible cell locations using edginess e) shrink the cell search space f) find cell locations g) Elimination of the nested cell locations h) cell locations output list

5.3. STAGE 2: Automated Cell Viability Analysis

Examiner's experience and tiredness substantially affects the accuracy throughout the manual observation of cell viability. The unsteady results of cell viability may end up with a biased observation results accordingly. Therefore, an automated decision-making system is inevitably needed to improve accuracy and consistency of the cell viability analysis. We investigate various combinations of classifiers and feature extractors (i.e. classification models) to maximize performance of automated viability analysis. The classification models are tested on novel image dataset which contains two types of cancer cell images, namely, caucasian promyelocytic leukemia (HL60), and chronic myelogenous leukemia (K562).

We conducted a series of benchmarking by the combination of various classifiers and feature extractors for the cell viability analysis. In this study, we employ three promising feature extractors, namely, LBP, LPQ, and HOG. Additionally, we cover a variety of supervised learning algorithms such as KNN, SVM, and RF which show superior performances in adverse number of classification tasks.

For this purpose, we theoretically and quantitatively investigate different texture, edge, color features and their combinations with three types of classifier to obtain the best configuration.

We were utilized the 3 fold, 5 fold, and 10 fold cross validation for the model classification error. There are various ways to estimate error for a given model. We utilize misclassification rate that is the average percentage of cases assigned to the wrong category in each fold.

5.4. STAGE 3: Overall Proposed Method

In this stage, we execute two consecutive decision procedures explained in Stage 1 (i.e. cell location finding pipeline) and Stage 2 (i.e. automated cell viability analysis), and obtain final cell locations as well as dead and alive cell numbers on a raw Hemocytometer image (Figure 33).

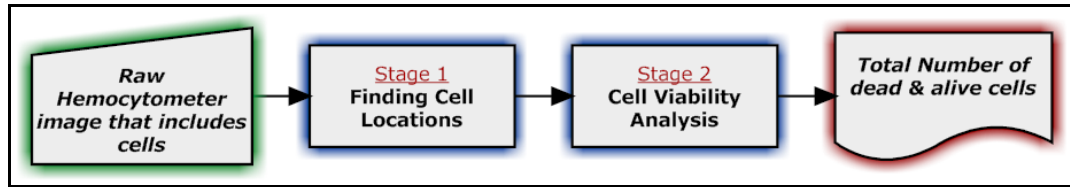


Figure 33. Proposed light microscope to vision based cell analyzer (Stage3)

For this purpose, we first apply Stage 1 to estimate the cell location on the image. This step intuitively obtains final results that comprise the possible cell location coordinates and the optimum window sizes which successfully cover the whole cells. Later, by using these decisions, we crop the possible cell locations and employ the mechanism proposed in Stage 2 to categorize the cells based on their distinct visual similarities to the dead and alive cell examples in the training set. We should note that since the performance of the overall system depends on these two procedures, the total error should be considered as additive sum of the error in both stages.

CHAPTER 6

EXPERIMENTAL RESULTS AND DISCUSSION

There are several statistical measures to evaluate the performance of the proposed approaches that help to compare with each other in terms of rigid standards.

6.1. Performance Metrics

In order to measure the performance of proposed method, confusion matrices [114] are formed. A Confusion matrix is the way of representing consistency of produced output results as tabular form. True positives (TP), true negatives (TN), false positives (FP), and false negatives (FN), are the four different possible outcomes of a single prediction for a two-class case. TP and TN are obviously correct classifications. FP is when the computed value is incorrectly classified as negative, when it is in fact positive. A FN is when the computed value is incorrectly classified as positive when it is in fact negative. Table 4 indicates a sample of confusion matrix including TP, FN, FP, and TN.

Table 4. Sample confusion matrix

| Actual | Predicted | |
|----------|-----------|----------|
| | Positive | Negative |
| Positive | TP | FN |
| Negative | FP | TN |

There are several statistical metrics depending on the created confusion matrix to evaluate the performance [115] of the proposed approaches that help to compare with each other in terms of rigid standards, namely, recall, precision, and F-score.

Recall is a function of TP and FN.

$$\text{recall} = \frac{\text{TP}}{\text{TP} + \text{FN}} \quad (9)$$

Precision is a function of TP and FP.

$$\text{precision} = \frac{\text{TP}}{\text{TP} + \text{FP}} \quad (10)$$

The F-score (F) is introduced as harmonic mean of recall and precision (or positive predictive value and sensitivity).

$$\text{F-score} = 2 \times \frac{\text{precision} \times \text{recall}}{\text{precision} + \text{recall}} \quad (11)$$

6.2. Method Performance Evaluation Routine

Before obtaining results, it requires a well-defined evaluation process that is repeatable, objective and depends on solid evaluation metrics. The benefit of following a standardized and comprehensive process is to have an opportunity to develop guidance for evaluation of future alternative method proposals. Also, this avoids the possible misjudgments.

Established evaluation process needs three entry lists, namely, ground truth, produced, and location those holds locations of expert labeled data, method generated data, and ROI edge data, respectively. Lists hold locations on rows formed as the bounding box (i.e. [x y with height]) which is explained earlier. Figure 34 presents the full evaluation workflow.

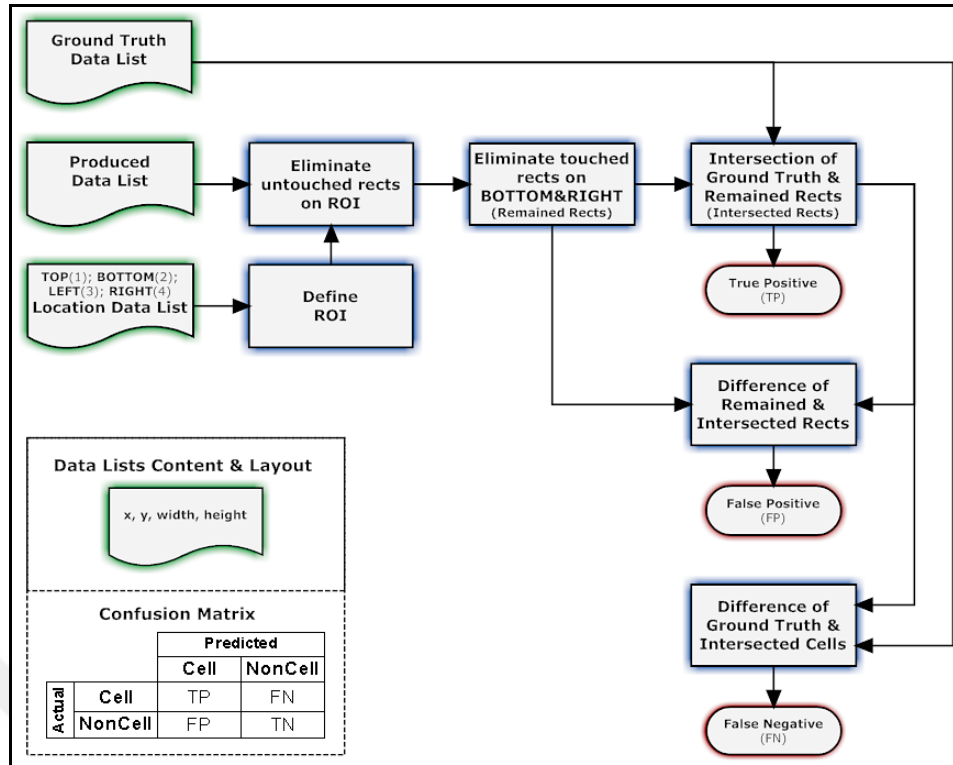


Figure 34. Method performance evaluation flow chart

When the process starts; first, untouched bounding boxes on ROI and touched bounding boxes on bottom and right ROI edges are eliminated. ROI has been determined using ROI edge data. Second, finding out count of collusion (i.e. intersection) occurrence between expert labeled data and method generated data as TP value which indicates the number of truly found cell locations. Last, investigation of non-collided (i.e. difference) instances depending on the order of lists which may be between expert labeled data and method generated data as FN or between method generated data and between expert labeled data as FN.

6.3. Proposed Cell Counting Pipeline Performance

In order to assess the capacity of the proposed method on the dataset, a series of analysis have been performed in the following section. Even if it is important to maintain the balance between speed and accuracy for a proposed method, this study preliminary considers the accuracy in terms of recall, precision, and f-score.

First, we utilize k-fold cross validation [116] to estimate the best performance between different feature extractors and classifiers by tuning related parameters

(Table 5) using cropped patch images (Table 2). Second, using the best combination parameters overall system performance is evaluated (Table 6 and Table 7) using our pipeline on the HL60_HEM40x_CC dataset. K-fold procedure begins with splitting corresponding total set into k subsets. Then, a test fold chooses from one of the k subsets and the remaining k-1 subsets are used for training on the each iteration. We changed the k value in order to 3, 5, 10, and 100 one by one. The results of k-fold are highly correlated and support each other. The highest emerged results are summarized on Table 5 as best pairs and fine tuning parameters.

We considered various parameters for tuning by feature extractors and classifiers. You can find the details of these methods in previous chapters. Since, LBP computes using N sampling points on a circle of radius R, examined values 2 to 8 by 2 and 4 to 6 by 4, accordingly. LPQ uses size of local window (WinSize) with 3 to 5 by 6 and low frequency estimation method (Frequentim), whether 1 for STFT with uniform window, 2 for STFT with Gaussian window or 3 for Gaussian derivative quadrature filter pair. HOG is evaluated by changing only cell size (CellSize) 6 to 32 by 2. KNN is tested by changing the size of k that 1 to 21 by 2 and defined when k equal 3 is the best choice. SVM is used linear or RBF kernel. RF is tested using fix 250 trees.

Table 5. The best parameters for cell location finding

| Classifier | LBP | | LPQ | | HOG |
|-----------------------|-----|----|---------|------------|----------|
| | R | N | Winsize | Frequentim | CellSize |
| KNN _(k=3) | 3 | 20 | 9 | 1 | 12 |
| SVM _{linear} | 3 | 4 | 17 | 3 | 12 |
| SVM _{rbf} | 3 | 4 | 17 | 2 | 18 |
| RF ₍₂₅₀₎ | 4 | 20 | 19 | 1 | 14 |

Experiments are conducted on our proposed dataset. All analyses were completed using a fixed set of parameters set that is defined previously for each feature extractors and classifiers (Table 4). Since HL60_HEM40X_CC consist of two distinct labeled set of images, one of the image set is used for training, meanwhile the performance is reported on other set and vice versa.

The experimental results are presented in Table 6 and Table 7 as a tabular form, the recall (9) and precision (10) percentages are obtained by comparing with the ground

truth for each image sets, depending on different ratio types and different thresholds. In addition, f-scores (11) are estimated as an extra evaluation metric. Table 6 presents results by using min type ratio with threshold 0.8. It means that 80% or more bounding box intersection area is reached between the method output and the expert annotation as explained in previous chapters. On the other hand, Table 7 reveals the result of proposed cell location finding method by min type ratio with 0.9 as threshold.

Table 6. Cell location finding results by Min Type bounding box with threshold 0.8

| Descriptor | Classifier | Set 1 | | | Set 2 | | |
|------------|-----------------------|--------|-----------|------|--------|-----------|------|
| | | Recall | Precision | F | Recall | Precision | F |
| LBP | KNN | 0.29 | 0.06 | 0.10 | 0.21 | 0.05 | 0.08 |
| | SVM _{linear} | 0.74 | 0.50 | 0.60 | 0.69 | 0.44 | 0.54 |
| | SVM _{rbf} | 0.79 | 0.53 | 0.63 | 0.70 | 0.47 | 0.56 |
| | RF | 0.75 | 0.48 | 0.59 | 0.73 | 0.48 | 0.58 |
| LPQ | KNN | 0.29 | 0.08 | 0.13 | 0.31 | 0.11 | 0.16 |
| | SVM _{linear} | 0.84 | 0.36 | 0.50 | 0.58 | 0.79 | 0.67 |
| | SVM _{rbf} | 0.85 | 0.56 | 0.68 | 0.74 | 0.62 | 0.67 |
| | RF | 0.91 | 0.75 | 0.82 | 0.86 | 0.76 | 0.81 |
| HOG | KNN | 0.54 | 0.40 | 0.46 | 0.67 | 0.58 | 0.62 |
| | SVM _{linear} | 0.94 | 0.51 | 0.66 | 0.93 | 0.66 | 0.77 |
| | SVM _{rbf} | 0.96 | 0.91 | 0.93 | 0.95 | 0.91 | 0.93 |
| | RF | 0.94 | 0.88 | 0.91 | 0.93 | 0.87 | 0.90 |

Table 7. Cell location finding results by Min Type bounding box with threshold 0.9

| Descriptor | Classifier | Set 1 | | | Set 2 | | |
|------------|-----------------------|--------|-----------|------|--------|-----------|------|
| | | Recall | Precision | F | Recall | Precision | F |
| LBP | KNN | 0.30 | 0.06 | 0.10 | 0.26 | 0.06 | 0.10 |
| | SVM _{linear} | 0.80 | 0.53 | 0.64 | 0.78 | 0.49 | 0.60 |
| | SVM _{rbf} | 0.85 | 0.57 | 0.68 | 0.80 | 0.53 | 0.64 |
| | RF | 0.89 | 0.58 | 0.70 | 0.87 | 0.57 | 0.69 |
| LPQ | KNN | 0.34 | 0.10 | 0.15 | 0.44 | 0.15 | 0.22 |
| | SVM _{linear} | 0.86 | 0.37 | 0.52 | 0.60 | 0.81 | 0.69 |
| | SVM _{rbf} | 0.86 | 0.57 | 0.69 | 0.75 | 0.63 | 0.68 |
| | RF | 0.93 | 0.78 | 0.85 | 0.89 | 0.78 | 0.83 |
| HOG | KNN | 0.67 | 0.49 | 0.57 | 0.80 | 0.69 | 0.74 |
| | SVM _{linear} | 0.98 | 0.53 | 0.69 | 0.97 | 0.93 | 0.95 |
| | SVM _{rbf} | 0.98 | 0.92 | 0.95 | 0.98 | 0.93 | 0.95 |
| | RF | 0.98 | 0.92 | 0.95 | 0.97 | 0.91 | 0.94 |

The results demonstrate that the HOG feature extraction approach is clearly more reliable than other popular methods such as LBP and LPQ. Furthermore, SVM with

RBF kernel and RF yield compatible success. KNN shows the worst performance and the performance drop reaches to 10%. Since, HOG is the best feature extractor; SVM with RBF kernel increases the overall recall and precision (i.e. f-score) to up to 3% compared to RF, up to 27% compared to a SVM with linear kernel, and up to 47% compared to KNN. In conclusion, the experimental results show that HOG and SVM combination with RBF kernel is the best performing approach on this dataset. That combination is reached up to 98%, 92%, and 95% interns of recall, precision, and f-score, respectively.

6.4. Proposed Automated Cell Viability Analysis Performance

In this section, we presented the experimental results for automated cell viability analysis by considering different sets of parameters for both feature extractors and classifiers. Each of this combination is called as a model. As a result, various problem specific observations have been introduced while comparing each model in terms of k-fold cross-validation misclassification rate. In the experiments, we tried different k values to assure the true characteristics of the models under various data variation.

For this purpose, through the benchmarking k value is set to 3, 5, and 10. However, in order to preserve the simplicity, we only consider 10-fold validation results since this analysis can yield more reliable results on the datasets. The parameters and their intervals (i.e. range) in the benchmark test are summarized in Table 8 and Table 9.

Table 8. Considered classifier parameters and intervals for automated cell viability analysis

| Values | Classifiers | | |
|-----------------|---------------------|-------------|-------------|
| | KNN | SVM | RF |
| Parameter | Number of neighbors | Kernel type | Forest size |
| <i>Interval</i> | 1:2:21 | Linear/rbf | 250 |

Table 9. Considered feature extractor parameters and intervals for automated cell viability analysis

| Values | Classifiers | | | | |
|-----------------|----------------------|---------------------|-----------------------------|--|---------------------|
| | LBP | | LPQ | | HOG |
| Parameter | Circle of radius “R” | Sampling points “N” | Local window size “winSize” | Local frequency estimation method “freestim” 1 → STFT - uniform window 2 → STFT - Gaussian window 3 → Gaussian derivative quadrature filter | Cell size “winsize” |
| <i>Interval</i> | 1:6 | 4:4:24 | 3:2:25 | | 6:2:36 |

For the experiments, two different cell image sets were utilized namely, HL60 and K562. The details of the sets are clarified in previous sections. Although each set contains different type and number of cell images, the same k-fold process is applied on both sets. The average size of the images is varied due to the cell type properties including, structural and dimensional variations.

When we compare HL60 and K562 cells in terms of size and morphology attributes, hl60 cells are relatively more circular and smaller than K562 ones. Additionally, the interior of the HL60 alive cells are clearer and transparent than the K562 alive cells. However, the dead cells show similar visual characteristics for both cell types. In the test and training phases, we fixed the dimension of the HL60 and K562 patch images to 72x72 and 90x90 respectively.

Moreover, the misclassification rates reported in all results can be varied between 0 and 1 where 0 indicates error-free while 1 means completely missed. Therefore, numerically lower error rate shows better performance in our experiments. Also, we used common graphical way of representation for the experimental results that is scatter plot to make more consistent analogy for all the combinations.

In order to preserve readability, we prefer to represent experimental results in figures from 22 to 27 by using markers as an indicator based on variation of the feature extractor parameters with respect to classifiers error. For each figure, horizontal axis represents the feature extractor parameter changes while the vertical axis represents

the misclassification rates. Additionally, each of the figures denotes KNN, SVM with linear kernel, SVM with rbf kernel and RF with different colors and markers, such as, black dash-dot line by cross marker, red dashed line by point marker, green solid line by Asterisk marker, and blue dotted line by plus sign marker, respectively. Lastly, the misclassification rate of KNN saturates when k equals three neighbors. Therefore, we fixed the value of k for our experiments as indicated Table 5.

We discussed the obtained experimental results into two cases: first we individually explained the results for each type of cells. Second, we strive to find general statements for the model by interpreting the results jointly on both of the cell types.

From Figure 35 to Figure 37, misclassification rate are presented for HL60 cell patch images. First observation is that the combination of KNN with LPQ yields the lowest error percentage by 0.0311%. RF achieves the second best performance with the LPQ. It reaches up to 0.0329% misclassification rate. KNN with LBP gives third best performance by 0.0399%. Lastly, SVM shows its minimum error on rbf kernel with HOG by 0.0423%. The worst performance is estimated by the combination of KNN and HOG as 0.1547%.

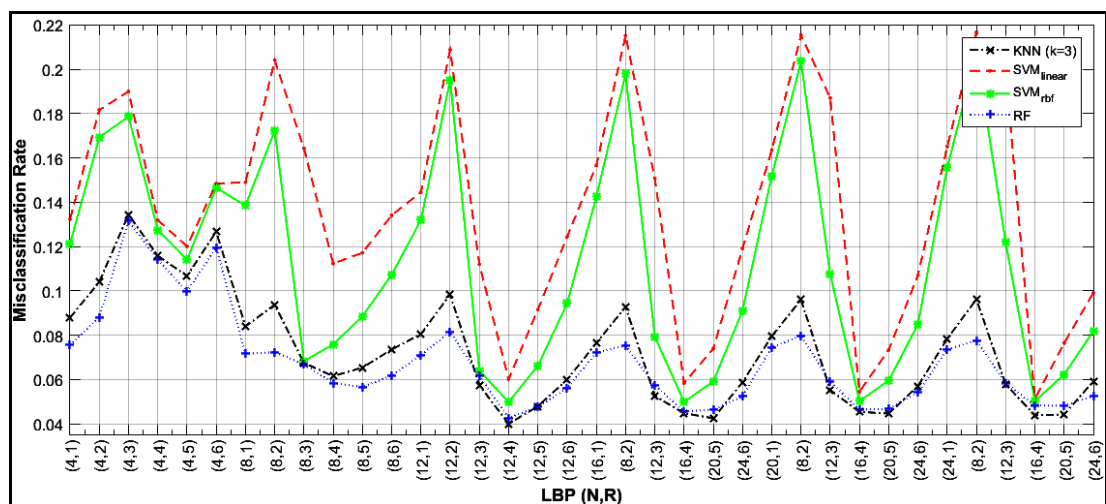


Figure 35. Misclassification rates for HL60 using various parameters of LBP

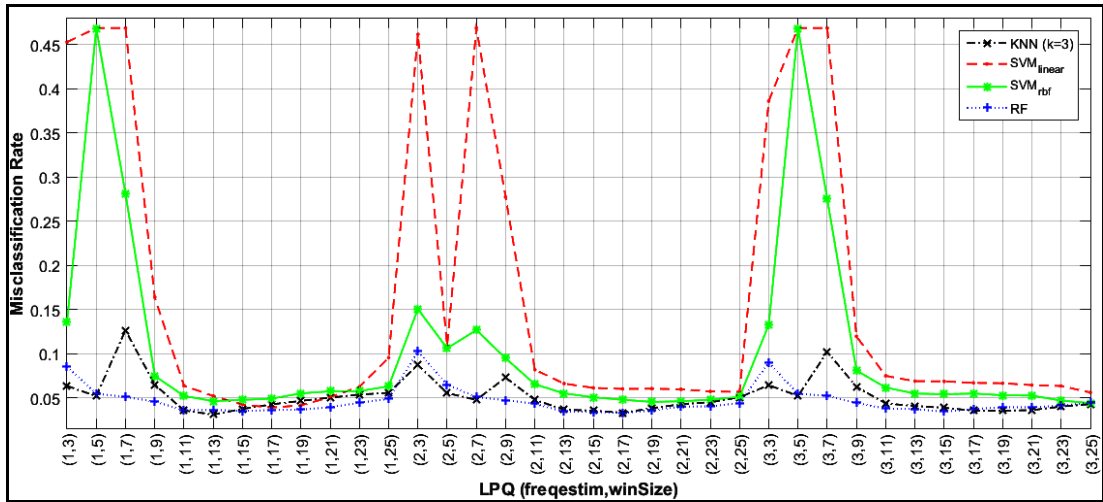


Figure 36. Misclassification rates for HL60 using various parameters of LPQ

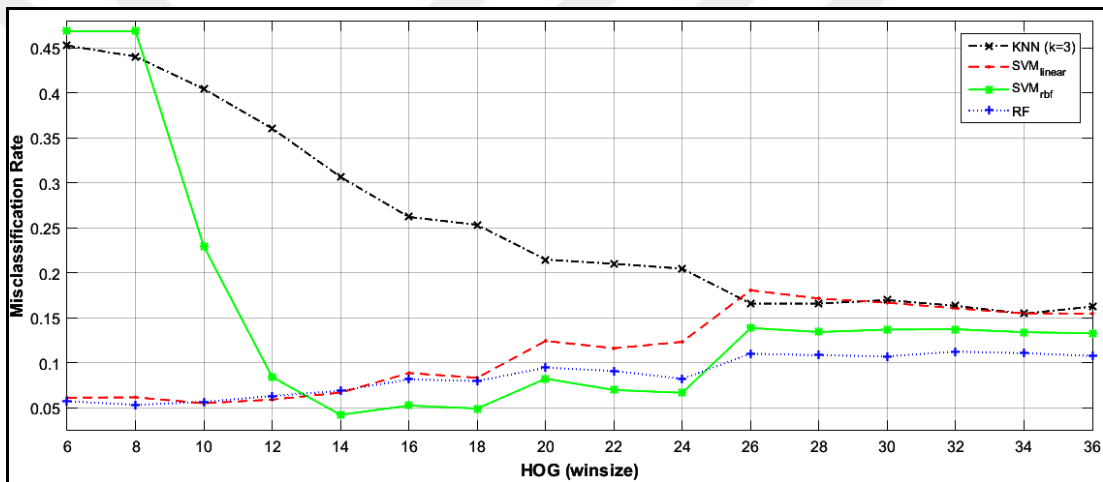


Figure 37. Misclassification rates for HL60 using various parameters of LBP

The experimental results on K562 cell patch images are summarized from Figure 38 to Figure 40. RF with LPQ obtains the lowest misclassification rate on this type of cell by 0.0824%. KNN is the second best performance with the LPQ and reaches the 0.0994%. Third best combination is achieved by SVM with rbf kernel and HOG as 0.1102%. SVM with linear kernel and LPQ yield the worst performance by 0.4922%.

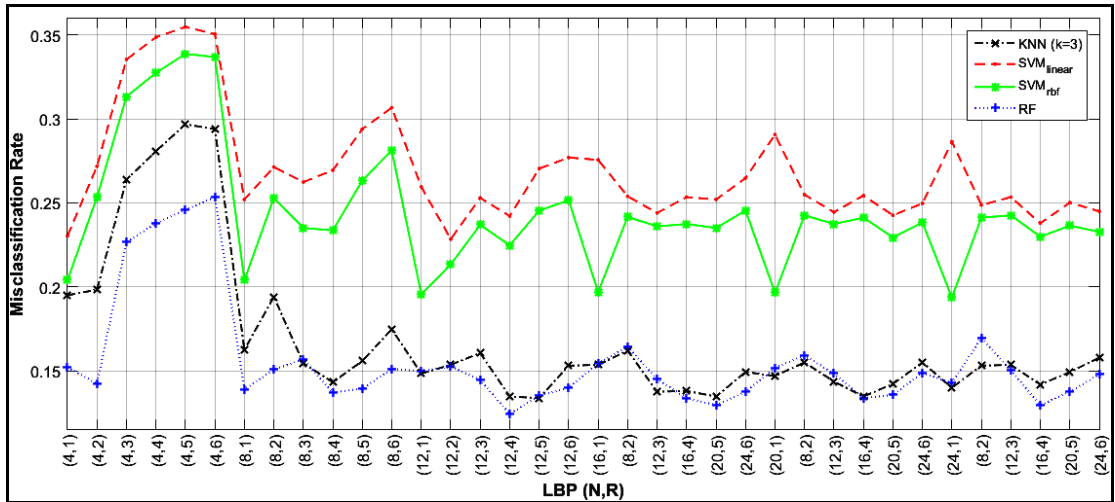


Figure 38. Misclassification rates for K562 using various parameters of LBP

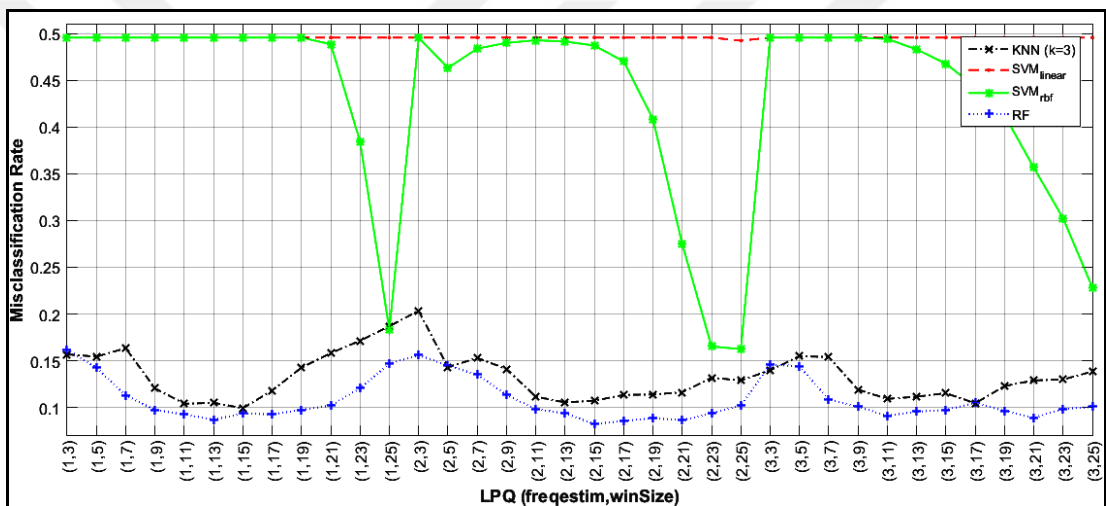


Figure 39. Misclassification rates for K562 using various parameters of LPQ

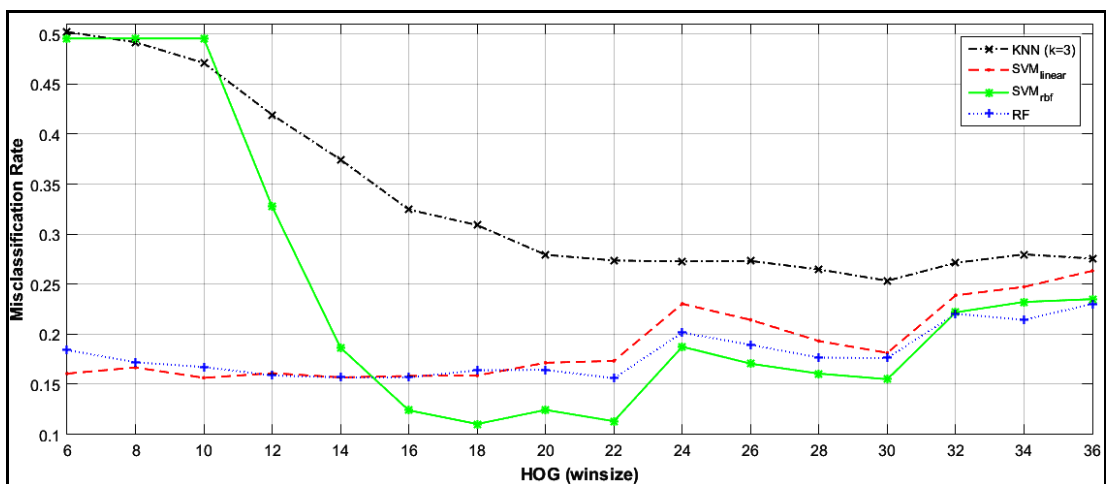


Figure 40. Misclassification rates for K562 using various parameters of HOG

To ease the understandability we illustrate the lowest experimental results in Table 10 and Table 11. In each table, first values in parentheses are indicates the optimum parameter for models. The second values show the obtained misclassification rates. Bold characters denote the lowest error rate estimated for each feature type while underlined value indicates the lowest error rate for each classifier.

Table 10. Obtained the lowest misclassification rates for HL60

| Features | Classifiers | | | |
|----------|---------------------------------|--------------------------|-------------------------------|--------------------------|
| | KNN | SVML | SVMR | RF |
| LBP | (12,4) 0.03998 | (16,4) 0.05123 | (12,4) 0.04987 | (12,4) 0.04269 |
| LPQ | (1,13) <u>0.03105</u> | (1,17) <u>0.03901</u> | (3,25) 0.04405 | (2,17) <u>0.03299</u> |
| HOG | (34) 0.1547 | (10) 0.05511 | (14) <u>0.04231</u> | (8) 0.05337 |

Table 11. Obtained the lowest misclassification rates for K562

| Features | Classifiers | | | |
|----------|--------------------------|-----------------------|------------------------------|---------------------------------|
| | KNN | SVML | SVMR | RF |
| LBP | (12,5) 0.1338 | (12,2) 0.2285 | (24,1) 0.1936 | (12,4) 0.1244 |
| LPQ | (1,15) <u>0.09939</u> | (2,25) 0.4922 | (2,25) 0.1625 | (2,17) <u>0.08243</u> |
| HOG | (30) 0.2534 | (10) <u>0.1564</u> | (18) <u>0.1102</u> | (22) 0.1559 |

As expected, the number of cell images can directly effect on model performance [117]. For our case, we have less number of K562 cell images compared to the HL60 cell images, thus average misclassification rate of K562 is higher than the HL60. When the experimental results of both sets are considered, the overall observations are made as follows:

- KNN and RF show relatively less misclassification rate with LBP and LPQ rather than HOG.
- SVM with rbf kernel are more accurate than SVM linear kernel.
- SVM has higher success with HOG than the other two feature extractor combinations, namely LBP and LPQ.
- RF has the lowest variance for all three feature extractors on both cell types.

6.5. Overall Method Results

Overall method structure is defined with the help of the experimental results that are obtained from previous stages. Experimentally, the most effective parameters are considered that will give the highest possible performance. In the first stage, the method parameters that showed superior success in cell location finding (i.e. cell counting) were used including, SVM with rbf kernel and HOG by 18x18 window size. In the second step, however, we considered two distinct classifiers along with a feature extractor that are KNN and RF for classifier with LBP as feature extractor. From here on, in all experimental results, these parameters are used when we refer to overall results.

Table 12 and Table 13 present overall results by using min type ratio with threshold 0.8. It means that 80% or more intersection (i.e. similarity) area between the method output and the expert annotation in terms of bounding boxes as explained in previous chapters. On the other hand, Table 14 and Table 15 show the result of overall method by min type ratio with threshold 0.9 (i.e. 90% or more intersection).

Table 12. Automated cell viability results for HL60 by Min Type bounding box with threshold 0.8

| Sets | Cell Location Finding | | Cell Viability | | | |
|-------|-----------------------|-----------|----------------|-----------|--------|-----------|
| | SVMrbf with HOG | | KNN | | RF | |
| | Recall | Precision | Recall | Precision | Recall | Precision |
| Set 1 | 0.97 | 0.89 | 0.92 | 0.99 | 0.95 | 0.96 |
| Set 2 | 0.97 | 0.90 | 0.89 | 0.98 | 0.94 | 0.97 |

Table 13. Automated cell viability results for K562 by Min Type bounding box with threshold 0.8

| Sets | Cell Location Finding | | Cell Viability | | | |
|-------|-----------------------|-----------|----------------|-----------|--------|-----------|
| | SVMrbf with HOG | | KNN | | RF | |
| | Recall | Precision | Recall | Precision | Recall | Precision |
| Set 1 | 0.89 | 0.81 | 0.80 | 0.94 | 0.83 | 0.94 |
| Set 2 | 0.88 | 0.79 | 0.83 | 0.90 | 0.88 | 0.93 |

Table 14. Automated cell viability results for HL60 by Min Type bounding box with threshold 0.9

| Sets | Cell Location Finding | | Cell Viability | | | |
|-------|-----------------------|-----------|----------------|-----------|--------|-----------|
| | SVMrbf with HOG | | KNN | | RF | |
| | Recall | Precision | Recall | Precision | Recall | Precision |
| Set 1 | 0.95 | 0.87 | 0.92 | 0.99 | 0.95 | 0.97 |
| Set 2 | 0.93 | 0.87 | 0.89 | 0.98 | 0.94 | 0.97 |

Table 15. Automated cell viability results for K562 by Min Type bounding box with threshold 0.9

| Sets | Cell Location Finding | | Cell Viability | | | |
|-------|-----------------------|-----------|----------------|-----------|--------|-----------|
| | SVMrbf with HOG | | KNN | | RF | |
| | Recall | Precision | Recall | Precision | Recall | Precision |
| Set 1 | 0.85 | 0.77 | 0.81 | 0.95 | 0.83 | 0.95 |
| Set 2 | 0.84 | 0.75 | 0.83 | 0.90 | 0.87 | 0.94 |

In Table 12, 13, 14 and 15, there are few common observations for cell viability and overall method performance. First, KNN achieves lower recall at high precision but RF reaches better recall at low precision. Since we choose higher recall as the indicator of success, we continue with the approach of higher recall.

Second, the cell location finding (stage 1) and the cell viability (stage 2) are consecutive stages. Therefore, to estimate the overall success, we need to multiply the individual success of each stage. In this manner, in Table 12, 13, 14 and 15, it's possible to say that our overall method reaches up to 92% and 74% in terms of recall scores for HL60 and K562 cancer cells, respectively, with the high precision.

Finally, overall recall and precision results are relatively lower for K562 cell images. As we mentioned earlier, the main reason for that is that the number of image quantity varies according to the cell type in our dataset. Since unsupervised approaches are adapted for the proposed method, the numerical differences affect the classifier performances. This issue has been discussed in many different publications in literature [118-120].

CHAPTER 7

CONCLUSIONS

This thesis proposes a reliable, inclusive, and adaptable conversational middleware software prototype to substitute manual cell counting as an automatic cell analyzer. The proposed method similarly uses a microscope and hemocytometer as in the manual counting while it eliminates the shortcomings of human labor and reliability. The tests are conducted on the most known cancer cell types namely, HL60 and K562. In the study, the method considers multidisciplinary research areas including; cell biology, computer vision, machine learning and software engineering. In the end, various observations have been made with the help of the experimental results.

To the best of our knowledge, there is no publicly available hemocytometer image dataset for cell counting and cell viability. First, we acquired two distinct novel data sets as baselines namely, HL60_HEM40x_CC and HL60_K512_HEM40X_CV that are publicly available for further academic researches. These datasets are released from the “biochem.atilim.edu.tr/datasets/” web address to make contribution to the image based cell counting and cell viability research fields.

HL60_HEM40x_CC is mainly prepared for cell counting, which includes total 468 raw hemocytometer images acquired on 40x light microscope magnification using unstained HL60 cells. Also, ground truth annotation labeled by experts comprises total 6890 cells. Moreover, HL60_K512_HEM40X_CV is collected for cell viability analysis. It contains two different subsets of stained cancer cell images as HL60 and K512.

Second, the state-of-the-art and generic pipeline is presented for the automated hemocytometer based cell counting that can be easily adapted to different cell types with slight parameter tuning. For this purpose, we conduct several experiments with different feature and classification approaches to obtain the best performing configuration. Intuitively, our method is primarily based on multi-scale sliding window that can be used for finding cell localization (i.e. cell counting). Our main aim is to propose a method that can be generalized to count different types of cells, by mainly focusing on HL60 cancer cells based on hemocytometer and it can be easily tuned with few parameters. This alternative solution outperforms the currently available automated cell counters in terms of cost while preserving the accuracy. Several well-known feature extractors and classifiers are combined to maximize the performance throughout the method. As a result of our experiments the pipeline reaches up to 98%, 92%, and 95% in terms of recall, precision, and f-score, respectively using SVM with RBF kernel and HOG combination.

Third, various feature extractors along with the classifiers are benchmarked to observe the performance of the automated cell viability analysis. Our methodology is well-structured, extensive, and based on k-fold cross validation technique which is proven for the model selection. Throughout this analysis, three feature extractor approaches such as LBP, LPQ, and HOG are combined with the three different classification algorithms, namely KNN, SVM, and RF. We performed benchmarking on our novel dataset: HL60_K512_HEM40X_CV. The experimental results showed that KNN and RF with LPQ can be powerful alternatives to the conventional manual cell viability analysis. The misclassification rates of these combinations are reached at most 0.031 and 0.082, respectively.

Finally, overall method proposed by combining previously proposed cell location finding pipeline and automated cell viability benchmark. From our experimental results, our overall method reaches up to 92% and 74% in terms of recall scores for HL60 and K562 cancer cells, respectively, with the high precision. The experimental results also validate that the proposed method can be a powerful alternative to the current cell counting approaches.

In our knowledge there have been no studies found as a comprehensive method for all adverse conditions on hemocytometer based cell counting field like cell shape deformation, image brightness differences and possible impurities caused by cell suspension.

Nevertheless, there is still unoccupied research vacancy for further studies related to cell location finding performance improvement. New extensions and improvements can be made on the currently recommended datasets in future studies by adding new cancer types or new microscopic objected images. Moreover, there might be further studies on our dataset to reduce the classification errors by adapting different machine learning and feature extraction approaches in automated cell viability analysis, although the current results yield promising level of success.

REFERENCES

- [1] C. J. Lovitt, T. B. Shelper, V. M. Avery, "Advanced cell culture techniques for cancer drug discovery", *Biology (Basel)*, vol. 3, no. 2, pp. 345-367, 2014.
- [2] F. Piccinini, A. Tesei, G. Paganelli, W. Zoli, A. Bevilacqua, "Improving reliability of live/dead cell counting through automated image mosaicing", *Comput. Methods Programs Biomed*, vol. 117, no. 3, pp. 448-463, 2014.
- [3] M. Usaj, D. Torkar, M. Kanduser, and D. Miklavcic, "Cell counting tool parameters optimization approach for electroporation efficiency determination of attached cells in phase contrast images", *Journal of Microscopy*, vol. 241, no. 3, pp. 303-314, 2011.
- [4] R. Seethala, P. Fernandes, Eds., *Handbook of Drug Screening*, Marcel Dekker Inc., New York, 2001.
- [5] F. Triaud, C. Darmon, Y. Cariou, N. Ferry, T. Leneel, D. Clenet, D. Morin, F. Fraudeau, D. Blanchard, A. Truchaud, "Evaluation of an automated cell culture incubator: the autocell 200", *Journal of the Association for Laboratory Automation*, vol. 8, pp. 87-95, 2003.
- [6] G. Fey, S. Klassen, S. Theriault, J. Krishnan, "Decontamination of a Worst-case Scenario Class II Biosafety Cabinet Using Vaporous Hydrogen Peroxide", *Applied Biosafety: Journal of the American Biological Safety Association*, vol. 15, no. 3, pp. 142-150, 2010.

- [7] D.S. Lin, F.Y. Huang, N.C. Chiu, H.A. Koa, H.Y. Hung, C.H. Hsu, W.S. Hsieh, D.I. Yang, "Comparison of hemocytometer leukocyte counts and standard urinalyses for predicting urinary tract infections in febrile infants", *Pediatric Infectious Disease Journal*, vol. 19, no. 3, pp. 223-227, 2010.
- [8] F. J. Dein, A. Wilson, D. Fischer, and P. Langenberg, "Avian Leucocyte Counting Using the Hemocytometer," *J. Zoo Wildl. Med.*, vol. 25, no. 3, pp. 432-437, 1994.
- [9] Y. S. Yang, D. K. Park, H. C. Kim, M.-H. Choi, J.-Y. Chai, "Automatic identification of human helminth eggs on microscopic fecal specimens using digital image processing and an artificial neural network", *IEEE Trans. Biomed. Eng.*, vol. 48, no. 6, pp. 718-730, 2001.
- [10] K. Stanislav, "Light Microscopy in Biological Research", *Biophysical Journal*, vol. 88, no. 6, p. 3741, 2005.
- [11] S.Y. Chang, K. Keogh, J. E. Lewis, J. E. Ryu, E. S. Yi, "Increased IgG4-positive plasma cells in granulomatosis with polyangiitis: a diagnostic pitfall of IgG4-related disease", *Int J Rheumatol*, p. 121702, 2012.
- [12] S. Iloki, A. Gil, L. Lewis, A. Rosas, A. Acosta, G. Rivera, J. Rubio, "Cell growth curves for different cell lines and their relationship with biological activities", *Int. J. Biotechnol Mol. Biol. Res.*, vol. 4, no. 4, pp. 60-70, 2013.
- [13] J. R. Masters, G. N. Stacey, "Changing medium and passaging cell lines", *Nat. Protoc.*, vol. 2, no. 9, pp. 2276-2284, 2007.
- [14] K. Ongena, C. Das, J. L. Smith, S. Gil, G. Johnston, "Determining Cell Number During Cell Culture Using the Scepter Cell Counter", *Journal of Visualized Experiments*, vol. 45 , e2204, 2010.
- [15] D. C. Herrera et al., "Validation of three viable-cell counting methods: Manual semi-automated and automated", *Biotechnol. Rep.*, vol. 7, pp. 9-16, 2015.
- [16] K.S. Louis, A.C. Siegel, "Cell viability analysis using trypan blue: manual and automated methods", *Methods Mol. Biol.*, vol. 740, pp. 7-12, 2011.
- [17] S. A. Altman, L. Randers, G. Rao, "Comparison of trypan blue dye exclusion and fluorometric assays for mammalian cell viability determinations", *Biotechnology Progress*, vol. 9, no. 6, pp. 671-674, 1993.
- [18] J. T. Camp, Y. Jing, J. Zhuang, J. F. Kolb, S. J. Beebe, J. Song, R. P. Joshi, S. Xiao, K. H. Schoenbach, "Cell death induced by subnanosecond pulsed electric fields at elevated temperatures", *IEEE Trans. Plasma Sci*, vol. 40, no. 10, pp. 2334-2347, 2012.
- [19] W. Strober, "Trypan blue exclusion test of cell viability", *Curr. Protoc. Immunol Ed J. E Coligan Al. Appendix 3:Appendix 3B*, 2001.

- [20] E. Lengyel, "Ovarian Cancer Development and Metastasis", *American Journal of Pathology*, vol. 177, no. 3, pp. 1053-1064, 2010.
- [21] H. Inaba, M. Greaves, C. G. Mullighan, "Acute Lymphoblastic Leukaemia", *Lancet*, vol. 381, no. 9881, pp. 1943-1955, 2013.
- [22] A. S. Narang, D. S. Desai, Anticancer drug development, In: L. Yi, R. I. Mahato eds. *Pharmaceutical Perspectives of Cancer Therapeutics*, New York, Springer, pp. 49-92, 2009.
- [23] G. Tafuri, P. Stolk, F. Trotta, M. Putzeist, H.G. Leufkens, R.O. Laing, M. D. Allegri, "How do the EMA and FDA decide which anticancer drugs make it to the market? A comparative qualitative study on decision makers' views", *Ann Oncol*, vol. 25, no. 1, pp. 265-269, 2014.
- [24] D. Zhang, G. Luo, X. Ding, C. Lu, "Preclinical experimental models of drug metabolism and disposition in drug discovery and development", *Acta Pharm. Sin. B*, vol. 2, no. 2, pp. 549-561, 2012.
- [25] V. G. Kokich, "In-vitro vs in-vivo materials research", *American Journal of Orthodontics and Dentofacial Orthopedics*, vol. 143, no. 4, p. S11, 2013.
- [26] M. Brown, C. Wittwer, "Flow cytometry: Principles and clinical applications in hematology", *Clin. Chem.*, vol. 46, no. 8, pp. 1221-1229, 2000.
- [27] L. C. Huang et al., "Validation of cell density and viability assays using Cedex automated cell counter", *Biologicals*, vol. 38, pp. 393-400, May 2010.
- [28] C. Catal and B. Diri, "A Systematic Review of Software Fault Prediction Studies", *Expert Systems with Application*, vol. 36, no. 4, pp. 7346-7354, 2009.
- [29] Q. Feng et. al., "An New Automatic Nucleated Cell Counting Method With Improved Cellular Neural Networks (ICNN)", in *Proc. Int. Workshop on Cellular Neural Networks and Their Applic.*, Aug. 2006.
- [30] D. C. Huang et. al., "A computer assisted method for leukocyte nucleus segmentation and recognition in blood smear images", *Journal of Systems and Software*, vol. 85, no. 9, pp. 2104-2118, 2012.
- [31] H. Tulsani, R. Gupta, R. Kapoor, "An Improved Methodology for Blood Cell Counting", *IEEE International Conference on Multimedia Signal Processing and Communication Technologies (IMPACT)*, pp. 88-92, Nov. 2013.
- [32] F. Scotti, "Automatic Morphological Analysis for Acute Leukemia Identification in Peripheral Blood Microscope Images", *IEEE International Conference on Computational Intelligence for Measurement Systems and Applications (CIMSA)*, pp. 96-101, July 2005.

- [33] F. Scotti, "Robust Segmentation and Measurements Techniques of White Cells in Blood Microscope Images", Proceedings of the IEEE Instrumentation and Measurement Technology Conference (IMTC), pp. 43-48, April 2006.
- [34] R. D. Labati V. Piuri, F. Scotti "ALL-IDB: the acute lymphoblastic leukemia image database for image processing", in Proc. Of the IEEE International Conference on Image Processing (ICIP) September 2011.
- [35] A. Hamouda et. al., "Automated Red Blood Cell Counting", International Journal of Computing science, vol. 1, no. 2, pp. 13-16, 2012.
- [36] J. Ge et. al., "A system for counting fetal and maternal red blood cells", IEEE Trans. on Biomed. Eng. vol. 61, no. 12, pp. 2823–2829, 2014.
- [37] U. Bottigli et. al., "A New Automatic System of Cell Colony Counting", International Journal of Mathematical and Computer Sciences, vol. 3, no. 4, 2007
- [38] S. D. Brugger et. al., "Automated counting of bacterial colony forming units on agar plates", PLoS ONE, vol. 7, no. 3, pp. e33695, 2012.
- [39] H. Ogawa et. al., "Noise-free accurate count of microbial colonies by time-lapse shadow image analysis", Journal of Microbiological Methods, vol. 91, no. 3, pp.420-428, 2012.
- [40] G. L. Masala et. al., "Automatic cell colony counting by region-growing approach", Il Nuovo Cimento C, vol. 30, no. 6, pp. 633–644, 2007.
- [41] P. J. Chiang et. al., "Automated counting of bacterial colonies by image analysis", Journal of Microbiological Methods, vol. 108, pp. 74–82, 2014.
- [42] B. Prasad et. al., "A High Throughput Screening Algorithm for Leukemia Cells", IEEE Canadian Conference on Electrical and Computer Engineering, Ottawa, pp. 2094-2097, 2006.
- [43] B. Prasad, and W. Badwy, "High Throughput Algorithm for Leukemia Cell Population Statistics on a Hemocytometer", IEEE Biomedical Circuits and Systems Conference, pp. 27-30, 2007.
- [44] C. R. M. Mauricio et. al., "Image-Based Red Cell Counting for Wild Animal Blood", Engineering in Medicine and Biology Society (EMBS), pp. 438-441, 2010.
- [45] Y. W. Chen, and P. J. Chiang, "Automatic Cell Counting for Hemocytometers through Image Processing", World Academy of Science, Engineering & Technology, vol. 58, p. 719, 2011.
- [46] F. Chobngam et. al., "Preliminary results of death cell counting based on K-mean clustering", Biomedical Engineering International Conference (BMEiCON), 2012.

- [47] D. Sui et. al., "Bright field microscopic cells counting method for BEVS using nonlinear convergence index sliding band filter", *BioMedical Engineering OnLine*, vol. 13, no. 147, 2014.
- [48] T. Gultekin, C. Koyuncu, C. Sokmensuer, C. Gunduz-Demir, "Two-tier tissue decomposition for histopathological image representation and classification", *IEEE Trans. Med. Imag.*, vol. 34, no. 1, pp. 275-283, 2015.
- [49] X. Yao, M.M. Gomes, M.S. Tsao, C.J. Allen, W. Geddie, H. Sekhon, "Fine-needle aspiration biopsy versus core-needle biopsy in diagnosing lung cancer: a systematic review", *Curr Oncol*, vol.19, no. 1, pp. e16-e27, 2012.
- [50] P. Wang, X. Hu, Y. Li, Q. Liu, X. Zhu, "Automatic cell nuclei segmentation and classification of breast cancer histopathology images", *Signal Process.*, vol. 122, pp. 1-13, 2016.
- [51] K. Sirinukunwattana, A. M. Khan, N. M. Rajpoot, "Cell words: Modelling the visual appearance of cells in histopathology images", *Comput. Med. Imag. Graph.*, vol. 42, pp. 16-24, 2015.
- [52] M. Kruk, S. Osowski, and R. Koktyisz, "Recognition and classification of colon cells applying the ensemble of classifiers", *Computers in Biology and Medicine*, vol. 39, no. 2, pp. 156–165, 2009.
- [53] V. V. Lyashenko, A. M. A. Babker, O. A. Kobylin, "The methodology of wavelet analysis as a tool for cytology preparations image processing", *Cukurova Medical Journal*, vol. 41, no.3, pp. 453-463, 2016.
- [54] L. J. Pribyl, K. A. Coughlin, T. Sueblinvong, K. Shields, Y. Iizuka, L. S. Downs, R. G. Ghebre, M. Bazzaro, "Method for obtaining primary ovarian cancer cells from solid specimens", *J. Vis. Exp.*, vol. 84, pp.e51581, 2014.
- [55] F. Triaud, D.-H. Clenet, Y. Cariou, T. Le Neel, D. Morin, A. Truchaud, "Evaluation of automated cell culture incubators", *J. Assoc. Lab. Autom.*, vol. 8, pp. 82-86, 2003.
- [56] K. Bora, M. Chowdhury, L. B. Mahanta, M. K. Kundu, and A. K. Das, "Automated classification of pap smear images to detect cervical dysplasia", *Computer Methods and Programs in Biomedicine*, vol. 138, pp. 31-47, 2017.
- [57] S. Nazlibilek, D. Karacor, K. L. Ertürk, G. Sengul, T. Ercan, F. Aliew, "White Blood Cells Classifications by SURF Image Matching, PCA and Dendrogram", *Biomedical Research*, vol. 26, no. 4, pp. 633-640, 2015.
- [58] D. K. Das et al., "Machine learning approach for automated screening of malaria parasite using light microscopic images", *Journal of Micron*, vol. 45, pp. 97-106, 2013.
- [59] S.D. Cataldo, E. Ficarra, "Mining textural knowledge in biological images: applications, methods and trends", *Comput. Struct. Biotechnol. J.*, vol. 15, 2017.

- [60] H. Irshad, A. Veillard, L. Roux, D. Racoceanu, "Methods for nuclei detection segmentation and classification in digital histopathology: A review Current status and future potential", *IEEE Rev. Biomed. Eng.*, vol. 7, pp. 97-114, 2014.
- [61] C. Sommer, D. W. Gerlich, "Machine learning in cell biology—Teaching computers to recognize phenotypes", *J. Cell Sci.*, vol. 126, pp. 5529-5539, 2013.
- [62] M. Saraswat, K.V. Arya, "Automated microscopic image analysis for leukocytes identification: a survey", *Micron*, vol. 65, pp. 20-33, 2014.
- [63] J. Rawat, A. Singh, H. S. Bhaduria, J. Virmani, "Review of Leukocyte Classification for Microscopic Blood Images", In *Proceedings of 2nd IEEE International Conference on Computing for sustainable Global Development, (IndiaCom-2015)*, New Delhi, pp. 1948-1954, March 2015.
- [64] M. A. Aswathy, M. Jagannath, "Detection of breast cancer on digital histopathology images: present status and future possibilities", *Informatics in Medicine Unlocked*, open access, In Press, 2016.
- [65] S. Beecham, N. Baddoo, T. Hall, H. Robinson, H. Sharp, "Motivation in Software Engineering: A Systematic Literature Review", *Information and Software Technology*, vol. 50, no. 9-10, pp. 860-878, 2008.
- [66] B. Kitchenham, O. Pearl Brereton, D. Budgen, M. Turner, J. Bailey, S. Linkman, "Systematic literature reviews in software engineering-A systematic literature review", *Information and Software Technology (IST)*, vol. 51, no. 1, pp. 7-15, 2009.
- [67] H.D. Mills, "The management of software engineering Part I: Principles of software engineering", *IBM Systems Journal*, vol. 19, no. 4, pp. 414-420, 1980.
- [68] T. Dingsøyr, S. Nerur, V. Balijepally, and N. B. Moe, "A decade of agile methodologies: Towards explaining agile software development", *J. Syst. Softw.*, vol. 85, no. 6, pp. 1213-1221, Jun. 2012.
- [69] C. Montabert, D. McCrickard, W. Winchester, M. Pérez-Quñones, "An integrative approach to requirements analysis: How task models support requirements reuse in a user-centric design framework", *Interacting with Computers*, vol. 21, pp. 304-315, 2009.
- [70] D. Pandey, U. Suman, A. K. Ramani, "An Effective Requirement Engineering Process Model for Software Development and Requirements Management", *Advances in Recent Technologies in Communication and Computing (ARTCom) 2010 International Conference on*, pp. 287-291, 2010.
- [71] M. Dabbagh, S. P. Lee, "An approach for integrating the prioritization of functional and nonfunctional requirements", *The Scientific World Journal*, 2014.

- [72] P. Hsia, D. Kung, and C. Sell, "Software requirements and acceptance testing," *Annals of software Engineering*, vol. 3, no. 1, pp. 291-317, 1997.
- [73] Nidhra Srinivas, Dondeti Jagruthi, "Black Box and White Box Testing Techniques —a literature review;," *International Journal of Embedded Systems and Applications (IJESA)*, vol. 2, no. 2, 2012.
- [74] P. Corke, "MATLAB toolboxes: Robotics and vision for students and teachers", *IEEE Robot. Autom. Mag.*, vol. 14, no. 4, pp. 16-17, 2007.
- [75] J.D. Musa and K. Okumoto, "Software Reliability Models: Concepts, Classification, Comparisons and Practice", *Electronic Systems Effectiveness and Life Cycle Costing*, Skvirzynski J.K. (ed.), NATO ASI Series, F3, Springer-Verlag, Heidelberg, pp. 395-424, 1993.
- [76] B. Boehm, "A Spiral Model of Software Development and Enhancement", *Computer*, vol. 21, no. 5, pp. 61-72, 1988.
- [77] D. G. Kafura, G. R. Reddy, "The Use of Software Complexity Metrics in Software Maintenance", *IEEE Transactions on Software Engineering*, vol. 13, no. 3, pp. 335-343, 1987.
- [78] S. Arora, B. Barak, *Computational Complexity: A Modern Approach*, Cambridge, U.K., Cambridge Univ. Press, 2009.
- [79] M. Sitaraman, G. Kuczycki, J. Krone, W. F. Ogden, A. Reddy, "Performance specification of software components", *Proc. Symp. Softw. Reusability: Putting Softw. Reuse Context*, pp. 3-10, May 2001.
- [80] S. F. Ding, H. Zhu, W. K. Jia, and C. Y. Su, "A survey on feature extraction for pattern recognition," *Artificial Intelligence Review*, vol. 37, no. 3, pp. 169–180, 2012.
- [81] G. Şengül, "Classification of parasite egg cells using gray level cooccurrence matrix and kNN", *Biomedical Research*, vol. 27, no. 3, pp. 829-834, 2016.
- [82] T. Ojala, M. Pietikäinen, D. Harwood, "A comparative study of texture measures with classification based on featured distributions", *Pattern Recog.*, vol. 29, no. 1, pp. 51-59, 1996.
- [83] T. Ojala, M. Pietikainen, T. Maenpaa, "Multiresolution Gray-Scale and Rotation Invariant Texture Classification with Local Binary Patterns", *IEEE Trans. Pattern Analysis and Machine Intelligence*, vol. 24, no. 7, pp. 971-987, 2002.
- [84] J. Shang, C. Chen, H. Liang and H. Tang, "Object recognition using rotation invariant local binary pattern of significant bit planes", *IET Image Processing*, vol. 10, no. 9, pp. 662-670, 2016.

- [85] V. Ojansivu, J. Heikkila, "Blur insensitive texture classification using local phase quantization", In: Proc. International Conference on Image and Signal Processing, pp. 236–243, 2008.
- [86] S. R. Zhou, P. J. Yin, M. J. Zhang, "Local binary pattern (LBP) and local phase quantization (LBQ) based on Gabor filter for face representation", Neurocomputing, vol. 116, pp. 260-264, 2013.
- [87] E. Rahtu, J. Heikkila, V. Ojansivu, T. Ahonen, "Local Phase Quantization for Blur-Insensitive Image Analysis", Image and Vision Computing, vol. 30, no. 8, pp. 501-512, 2012.
- [88] J. Heikkila, V. Ojansivu, E. Rahtu, "Improved blur insensitivity for decorrelated local phase quantization", in International Conference on Pattern Recognition. IEEE, pp. 818-821, Aug. 2010.
- [89] N. Dalal, B. Triggs, "Histograms of Oriented Gradients for Human Detection", Proc. IEEE Conf. Computer Vision and Pattern Recognition (CVPR), pp. 886-893, June 2005.
- [90] A. Chayeb, N. Ouadah, Z. Tobal, M. Lakrouf, O. Azouaoui, "HOG based multi-object detection for urban navigation", in 17th International IEEE Conference on Intelligent Transportation Systems (ITSC), pp. 2962-2967, Oct 2014.
- [91] B. Kotsiantis, "Supervised machine learning: a review of classification techniques", Informatica, vol. 31, no. 3, pp. 249-268, 2007.
- [92] D. Elizondo, "The linear separability problem: Some testing methods", IEEE Trans. Neural Netw., vol. 17, no. 2, pp. 330-344, Mar. 2006.
- [93] G. Guo, H. Wang, D. Bell, Y. Bi, K. Greer, "KNN model-based approach in classification", On the Move to Meaningful Internet Systems 2003: CoopIS DOA and ODBASE, pp. 986-996, 2003.
- [94] V. Anitha, S. Murugavalli, "Brain tumour classification using two-tier classifier with adaptive segmentation technique", IET Computer Vision, vol. 10, no. 1, pp. 9-17, 2016.
- [95] C. Cortes, V. Vapnik, "Support-vector networks", Machine learning, vol. 20, pp. 273-297, 1995.
- [96] A. Statnikov, L. Wang, C. Aliferis, "A comprehensive comparison of random forests and support vector machines for microarray-based cancer classification", BMC BIOINF, vol. 9, no. 1, pp. 319, 2008.
- [97] L. Zhao, K. Li, J. Yin, Q. Liu, S. Wang, "Complete three-phase detection framework for identifying abnormal cervical cells", IET Image Processing, vol. 11, no. 4, pp. 258-265, 2017.

- [98] J. Umamaheswari, G. Radhamani, "Quadratic program Optimization using Support Vector Machine for CT Brain Image Classification", *International Journal of Computer Science Issues*, vol. 9, no. 4, pp. 305-310, 2012.
- [99] A. Ben-Hur, C. Ong, S. Sonnenburg, B. Scholkopf, G. Ratsch, "Support Vector Machines and Kernels for Computational Biology", *PLoS Computational Biology*, vol. 4, no. 10, pp. 1-10, 2008.
- [100] L. Breiman, J. Friedman, R. Olshen, C. Stone, *Classification and Regression Trees*. New York, NY, USA: Wadsworth and Brooks, 1984.
- [101] L. Breiman, "Random forests", *Mach. Learn.*, vol. 45, no. 1, pp. 5-32, 2001.
- [102] R. Timofeev, *Classification and Regression Trees (CART) theory and applications*, Thesis (Masters) Berlin: Humboldt University, Center of Applied Statistics and Economics, 2004.
- [103] D. H. Wolpert, W. G. Macready, "No free lunch theorems for optimization", *IEEE Trans. Evol. Comput.*, vol. 1, no. 1, pp. 67-82, 1997.
- [104] C. Schaffer, "Selecting a classification method by cross-validation", *Machine Learning*, vol. 13, no. 1, pp. 135-143, 1993.
- [105] F. Tadayoshi, "Estimation of prediction error by using K-fold cross-validation", *Statistics and Computing*, vol. 21, no. 2, pp. 137-146, 2011.
- [106] C. H. Lampert, M. B. Blaschko, T. Hofmann, "Beyond Sliding Windows: Object Localization by Efficient Subwindow Search", *Proc. IEEE Conf. Computer Vision and Pattern Recognition (CVPR)*, June 2008.
- [107] Y. Wang, Y. Hu, J. Fan, Y. Zhang, Q. Zhang, "Collision Detection Based on Bounding Box for NC Machining Simulation", *Physics Procedia*, vol. 24, pp. 247-252, 2012.
- [108] B. S. Isgor, Y. G. Isgor, "Effect of Alpha-1-Adrenoceptor Blocker on Cytosolic Enzyme Targets for Potential use in Cancer Chemotherapy" *Int. J. Pharmacol* vol.8, no.5, pp. 333-343, 2012.
- [109] G. D. Birnie, "The HL60 cell line: a model system for studying human myeloid cell differentiation", *Br. J. Cancer Suppl.*, Vol.9, pp.41-45, 1988.
- [110] X. Z. Zhang, A. H. Yin, D. J. Lin, X. Y. Zhu, Q. Ding, C. H. Wang, Y. X. Chen, "Analyzing gene expression profile in K562 cells exposed to sodium valproate using microarray combined with the connectivity map database", *J. Biomed Biotechnol* , pp. 654291, 2012.
- [111] A. Saleem et. al., "Image fusion-based contrast enhancement", *EURASIP Journal on Image and Video Processing*, vol. 2012, no. 10, pp.1-17, 2012.

- [112] J. Canny, "A Computational Approach to Edge Detection", IEEE Transactions on Pattern Analysis and Machine Intelligence, vol. PAMI-8, no. 6, pp. 679-698, 1986.
- [113] R. Rothe et. al., "Non-maximum suppression for object detection by passing messages between windows", in Asian Conference on Computer Vision (ACCV), pp. 290-306, 2014.
- [114] M. Sokolova, G. Lapalme, "A systematic analysis of performance measures for classification tasks", Inf. Process. Manag., vol. 45, no. 4, pp. 427-437, Jul. 2009.
- [115] L. Zhao, K. Li, J. Yin, Q. Liu, S. Wang, "Complete three-phase detection framework for identifying abnormal cervical cells", IET Image Processing, vol. 11, no. 4, pp. 258-265, 2017.
- [116] R. Kohavi, "A study of cross-validation and bootstrap for accuracy estimation and model selection, " in Proc. 14th Int. Joint Conf. Artificial Intelligence, pp. 338-345, 1995.
- [117] D. Brain, G. I. Webb, "On the effect of data set size on bias and variance in classification learning", Proc. Australian Knowledge Acquisition Workshop (AKAW-99), pp. 117-128, 1999.
- [118] C. Catal, B. Diri, "Investigating the effect of dataset size metrics sets and feature selection techniques on software fault prediction problem", Inf. Sci., vol. 179, no. 8, pp. 1040-1058, 2009.
- [119] A. Krizhevsky, I. Sutskever, G. Hinton, "ImageNet Classification with Deep Convolutional Neural Networks", Proc. Neural Information and Processing Systems (NIPS), pp. 1097-1105, 2012.
- [120] C. Beleites, U. Neugebauer, T. Bocklitz, C. Krafft, J. Popp, "Sample size planning for classification models", Anal. Chim. Acta, vol. 760, pp. 25-33, 2013.